Atmos. Chem. Phys., 21, 13269–13286, 2021
https://doi.org/10.5194/acp-21-13269-2021

Atmospheric Chemistry and Physics
Open Access
EGU

Ammonium nitrate promotes sulfate formation through uptake kinetic regime

Yongchun Liu[1,5], Zemin Feng[1], Feixue Zheng[1], Xiaolei Bao[2,7], Pengfei Liu[3], Yanli Ge[3], Yan Zhao[3], Tao Jiang[4], Yunwen Liao[5], Yusheng Zhang[1], Xiaolong Fan[1], Chao Yan[6], Biwu Chu[3,6], Yonghong Wang[6], Wei Du[6], Jing Cai[6], Federico Bianchi[6], Tuukka Petäjä[6,8], Yujing Mu[3], Hong He[3], and Markku Kulmala[1,6]

[1]Aerosol and Haze Laboratory, Advanced Innovation Center for Soft Matter Science and Engineering, Beijing University of Chemical Technology, Beijing, 100029, China
[2]Hebei Provincial Academy of Environmental Sciences, Shijiazhuang, 050037, China
[3]State Key Joint Laboratory of Environment Simulation and Pollution Control, Research Center for Eco-Environmental Sciences, Chinese Academy of Sciences, Beijing, 100085, China
[4]Hebei Provincial Meteorological Technical Equipment Center, Shijiazhuang, 050021, China
[5]College of Chemistry and Chemical Engineering, China West Normal University, Nanchong, 637002, China
[6]Institute for Atmospheric and Earth System Research/Physics, Faculty of Science, University of Helsinki, P.O. Box 64, 00014, Finland
[7]Hebei Chemical & Pharmaceutical College, Shijiazhuang, 050026, China
[8]Joint International Research Laboratory of Atmospheric and Earth System Sciences (JirLATEST), University of Helsinki and Nanjing University, Nanjing 210023, China

Correspondence: Yongchun Liu (liuyc@buct.edu.cn) and Xiaolei Bao (bxl5@163.com)

Received: 5 April 2021 – Discussion started: 7 May 2021
Revised: 30 July 2021 – Accepted: 2 August 2021 – Published: 7 September 2021

Abstract. Although the anthropogenic emissions of SO_2 have decreased significantly in China, the decrease in SO_4^{2-} in $PM_{2.5}$ is much smaller than that of SO_2. This implies an enhanced formation rate of SO_4^{2-} in the ambient air, and the mechanism is still under debate. This work investigated the formation mechanism of particulate sulfate based on statistical analysis of long-term observations in Shijiazhuang and Beijing supported with flow tube experiments. Our main finding was that the sulfur oxidation ratio (SOR) was exponentially correlated with ambient RH in Shijiazhuang ($SOR = 0.15 + 0.0032 \times \exp(RH/16.2)$) and Beijing ($SOR = -0.045 + 0.12 \times \exp(RH/37.8)$). In Shijiazhuang, the SOR is linearly correlated with the ratio of aerosol water content (AWC) in $PM_{2.5}$ ($SOR = 0.15 + 0.40 \times AWC/PM_{2.5}$). Our results suggest that uptake of SO_2 instead of oxidation of S(IV) in the particle phase is the rate-determining step for sulfate formation. NH_4NO_3 plays an important role in the AWC and the change of particle state, which is a crucial factor determining the uptake kinetics of SO_2 and the enhanced SOR during haze days. Our results show that NH_3 significantly promoted the uptake of SO_2 and subsequently the SOR, while NO_2 had little influence on SO_2 uptake and SOR in the presence of NH_3.

1 Introduction

Atmospheric particulate matter (PM) is a worldwide concern due to its adverse effect on human health, such as its association with respiratory and cardiovascular diseases, lung cancer, and premature death (WHO, 2013; Lelieveld et al., 2015). The Chinese government has made great efforts to improve the air quality (Cheng et al., 2019). For example, the annual $PM_{2.5}$ concentration in Beijing decreased from 89.5 $\mu g\,m^{-3}$ in 2013 to 58 $\mu g\,m^{-3}$ in 2017 due to the stringent reduction of local and regional emissions (Cheng et al., 2019; Ji et al., 2019). However, the $PM_{2.5}$ concentrations in most regions of China (Cheng et al., 2019; Q. Chen et al., 2019; Huang et al., 2019; Tian et al., 2019) are still significantly higher than the $PM_{2.5}$ standard recommended by

the World Health Organization (WHO) (WHO, 2006). Haze events also occur with high frequency, especially, in autumn and winter.

Secondary inorganic aerosol (SIA) including sulfate (SO_4^{2-}), nitrate (NO_3^-), ammonium (NH_4^+) and secondary organic aerosol (SOA) usually contribute to $\sim 70\,\%$ of $PM_{2.5}$ mass concentration in different regions (Huang et al., 2014; An et al., 2019). SIA often accounts for more than a half of $PM_{2.5}$ mass in severe pollution events (Zheng et al., 2015; Wang et al., 2016). Even SO_4^{2-} exceeds more than 20 % of $PM_{2.5}$ mass (Guo et al., 2014; Wang et al., 2016; Xie et al., 2015; He et al., 2018). Interestingly, the anthropogenic emissions of SO_2 in 2017 reduced by $\sim 90\,\%$ when compared with 2000 in Beijing (Cheng et al., 2019; Lang et al., 2017). However, the decrease rate of particulate SO_4^{2-} concentration (Lang et al., 2017; C. Li et al., 2017) is much smaller than SO_2 (Lang et al., 2017; Zhang et al., 2020; Liu et al., 2021). For example, the annual mean concentration of SO_4^{2-} decreased by $0.1\,\mu g\,m^{-3}\,yr^{-1}$ from 2000 to 2013, followed by $1.9\,\mu g\,m^{-3}\,yr^{-1}$ from 2013 to 2015 in Beijing, while it decreased by $3.8\,\mu g\,m^{-3}\,yr^{-1}$ for SO_2 (Lang et al., 2017). This implies an enhanced oxidation rate of SO_2 in the atmosphere (Lang et al., 2017). However, the mechanisms and kinetics of particulate SO_4^{2-} formation in the real atmosphere are still open questions in many regions of China although they have been extensively discussed (Ervens, 2015; Warneck, 2018).

Particulate SO_4^{2-} can be formed through homogeneous oxidation of SO_2 by hydroxyl radicals (OH) and stabilized Criegee intermediates (SCIs) in the gas phase and subsequent uptake onto particles, while the OH pathway is the dominant gas-phase oxidation pathway (Seinfeld and Pandis, 2006; L. Liu et al., 2019). Modeling studies greatly underestimated ($\sim 54\,\%$) SO_4^{2-} concentration in serve pollution events in Beijing if only considering gas-phase oxidation of SO_2, while the normalized mean bias (NMB) decreased significantly after heterogeneous oxidation of SO_2 being considered (Zheng et al., 2015). Several heterogeneous and/or multiphase oxidation pathways, such as oxidation of SO_2 or sulfite by H_2O_2 (Huang et al., 2015; Maaß et al., 1999; P. Liu et al., 2020; Ye et al., 2021; Liu et al., 2021), HONO (J. F. Wang et al., 2020), and O_3 (Maahs, 1983) or photochemical oxidation of SO_2 (Yu et al., 2017; Xie et al., 2015), catalytic oxidation of SO_2 by transition metal ions (TMI) (Warneck, 2018; Martin and Good, 1991; Wang et al., 2021) and oxidation of SO_2 by NO_2 (He et al., 2014; Clifton et al., 1988; Wang et al., 2016; Cheng et al., 2016; Wu et al., 2019; Spindler et al., 2003) in aqueous phase and heterogeneous oxidation of SO_2 on black carbon (Zhao et al., 2017; Zhang et al., 2020; Yao et al., 2020), have been proposed based on field measurements and laboratory and modeling studies. However, the relative contribution of these pathways to the SO_4^{2-} production is still controversial. For example, the contribution of heterogeneous oxidation to SO_4^{2-} production had been evaluated to be $(48 \pm 5)\,\%$ based on oxygen isotopic measurements (He et al., 2018), while it was 31 % even in the nighttime calculated by an observation-based modeling (OBM) (Xue et al., 2016). Gas-phase oxidation by OH could explain 33 %–36 % of SO_4^{2-} production in the Beijing–Tianjin–Hebei region (L. Liu et al., 2019), while it was negligible based on isotopic measurements (He et al., 2018) and OBM simulations (Xue et al., 2016). As for the oxidation of S(IV) species, which includes SO_2, HSO_3^- and SO_3^{2-}, in aqueous phase, oxidation by H_2O_2 (T. Liu et al., 2020; P. Liu et al., 2020; Ye et al., 2021), NO_2 (J. F. Wang et al., 2020; Wang et al., 2016; Cheng et al., 2016), O_3 (Fang et al., 2019), or TMI (Mn^{2+}) (Wang et al., 2021) was proposed as the most important pathway by different researchers. However, the relative importance of these oxidation paths varied greatly among different researches. For instance, TMI-catalyzed oxidation could explain $\sim 69\,\%$ of aqueous sulfate formation in North China Plain based on isotopic measurements and modeling (Shao et al., 2019), while oxidation by NO_2 or O_2 was the dominant oxidation path (66 %–73 %) based on isotopic measurements in another study (He et al., 2018). It should be noted that some reaction mechanisms mentioned above were proposed based on case studies in short-term observations. Thus, long-term observations at different environments are required to verify whether these mechanisms are statistically important. In addition, the previous studies mainly focused on oxidation process of SO_2 in particle phase, while it is unclear what are the controlling factors of the S(IV)-to-S(VI) conversion from the gas phase to the particle phase. In particular, it has been found that the mass fraction of NO_3^- and NH_4^+ is increasing gradually (Lang et al., 2017; Li et al., 2018). This will modify its physical properties, such as morphology, phase-state and so on. The feedback between aerosol physics and aerosol chemistry is still poorly understood.

In this work, 1-year field observations have been performed in Shijiazhuang and Beijing, synchronously. The formation mechanism of particulate sulfate has been statistically investigated to identify the controlling factors. The role of mass transfer of SO_2 and the oxidation of S(IV) in particle phase have been discussed based on flow tube experiments and field measurements. The conversion ratio of SO_2 to sulfate is statistically and linearly correlated to the aerosol water content (AWC), which is strongly modulated by particulate ammonium nitrate. The reaction kinetics and other factors affecting sulfate production have also been discussed.

2 Material and methods

2.1 Field measurements

Field measurements were performed at Shijiazhuang University (SJZ; 38.0281° N, 114.6070° E) and the west campus of Beijing University of Chemical Technology (BUCT; 39.9428° N, 119.2966° E) from 15 March 2018 to

15 April 2019. The SJZ station is on a rooftop of the main teaching building (5 floors, ∼ 23 m above the surface), which is around 250 m from the Zhujiang Road of Shijiazhuang. The BUCT station is on a rooftop of the main building (5 floors, ∼ 18 m above the surface), which is around 550 m from the 3rd Ring Road of Beijing. The distance between the two stations, which are the representative cities of Beijing-Tianjin-Hebei (BTH), is 260 km (Fig. S1). Both stations are surrounded by traffic and residential emissions, thus, are typical urban observation sites. The details about the observation stations have been described in our previous work (Y. Liu et al., 2020c, b, a).

Ambient air was drawn from the roof of the corresponding building. At the SJZ station, the mass concentration of $PM_{2.5}$ was measured by a beta attenuation mass monitor (BAM-1020, Met One Instruments, USA) with a smart heater (model BX-830, Met One Instruments Inc., USA) to control the RH of the incoming air to 35 % and a $PM_{2.5}$ inlet (URG) to cut off the particles with diameter larger than 2.5 µm. Particle-phase total concentrations of iron and manganese were measured using a heavy-metal analyzer (EHM-X100, Skyray Instrument). Water-soluble ions (Na^+, K^+, Mg^{2+}, Ca^{2+}, NH_4^+, SO_4^{2-}, Cl^- and NO_3^-) in $PM_{2.5}$ and gas pollutants (HCl, HONO, HNO_3, SO_2 and NH_3) were measured using an analyzer for monitoring aerosols and gases (MARGA, ADI 2080, Applikon Analytical B.V., the Netherlands) with 1 h of time resolution. At the BUCT station, the mass concentration of $PM_{2.5}$ was the mean concentration obtained from four surrounding monitoring stations (including Wanliu, Gucheng, Wanshouxigong and Guanyuan) of China Environmental Monitoring Centre (http://www.cnemc.cn, last access: 31 December 2020). The chemical composition of $PM_{2.5}$ was measured using a time-of-flight aerosol chemical speciation monitor (ToF-ACSM, Aerodyne) after the ambient air went through a $PM_{2.5}$ inlet (URG) and a Nafion dryer (MD-700-24, Perma Pure). The configuration and the operation protocol of ToF-ACSM have been described in previous work (Fröhlich et al., 2013). The ionization efficiency (IE) calibration for ACSM was performed using 300 nm dry NH_4NO_3 every month. Ambient air was drawn from the roof using a Teflon sampling tube (BMET-S, Beijing Saak-Mar Environmental Instrument Ltd.) with the residence time <10 s for gas-phase pollutant measurements. Trace gases including NO_x, SO_2, CO and O_3 were measured with the corresponding analyzer (Thermo Scientific, 42i, 43i, 48i and 49i) at both the SJZ and BUCT stations. Meteorological parameters including temperature, pressure, relative humidity (RH), wind speed and wind direction were measured using weather stations (WXT 520 at HAS/SJZ station and AWS 310 at AHL/BUCT station, Vaisala).

2.2 Uptake kinetics of SO_2 on dust internally mixed with NH_4NO_3

To understand the influence of RH on uptake kinetics (γ_{SO_2}), the γ_{SO_2} on dust internally mixed with NH_4NO_3 was measured using a coated-wall flow tube reactor. The configuration of the reactor and data process protocol have been described in detail previously (Han et al., 2013; Liu et al., 2015). The γ parameter, presenting the mass transfer kinetic of gas-phase SO_2 to particle phase, is defined by the net loss rate of SO_2 per collision onto the surface (Ravishankara, 1997; Usher et al., 2003), namely,

$$\gamma_{obs} = \frac{-\frac{dc}{dt}}{\omega} = \frac{2k_{obs}r_{tube}}{<c>}, \quad (1)$$

where $-dc/dt$ is the net loss rate of SO_2 when the surface is exposed to SO_2 (molecules s^{-1}); ω is the collision frequency (s^{-1}); k_{obs}, r_{tube}, and $<c>$ are the first-order rate constant of SO_2, the flow tube radius, and the average molecular velocity of SO_2, respectively. A correction for gas-phase diffusion limitations was considered for γ_{obs} calculations using the Cooney–Kim–Davis (CKD) method (Cooney et al., 1974; Murphy and Fahey, 1987). The Brunauer–Emmett–Teller (BET) uptake coefficient ($\gamma_{SO_2,BET}$) was obtained from the mass dependence of γ_{obs} as follows (Han et al., 2013; Liu et al., 2015):

$$\gamma_{SO_2,BET} = [\text{slope}]\frac{A_g}{S_{BET}}, \quad (2)$$

where [slope] is the slope of the plot of γ_{obs} versus the sample mass in the linear regime (mg^{-1}), A_g is the inner surface area of the sample tube (cm^2) and S_{BET} is the specific surface area of the particle sample ($cm^2\ mg^{-1}$).

Similar to a previous work (Zhang et al., 2019), dust internally mixed with NH_4NO_3 was used in the kinetics study, because it was difficult to deposit enough real ambient particles onto the inner surface of the sample holder. Although the composition of the model particles is much simpler than that of ambient particles, it is still meaningful, because we mainly focused on the influence of RH or aerosol water content (AWC) on uptake kinetics of SO_2. The mixture (mass ratio = 2 : 1) of A1 ultrafine test dust (Powder Technology Inc.) and NH_4NO_3 (AR, Sinopharm Chemical Reagent Co. Ltd, China) were suspended in the mixture of ethanol and water ($v : v = 1 : 3$). The inner surface of the Pyrex quartz tube (sample holder) was uniformly coated by the above mixture and dried overnight in an oven at 393 K. The sample mass was calculated according to the weighted mass of the dry tube before and after coating. NH_4NO_3 in the mixture was further confirmed using an ion chromatograph (Ω Metrohm 940, Applikon Analytical B.V., the Netherlands). Around 50 % of the NH_4NO_3 remained in the mixture even after heating and potential evaporation. To avoid the wall loss of SO_2 on the sample holder, all the inner surface of the

sample holder was covered with particles. The wall loss of SO_2 on the remained surface (the inner surface of the outside tube and the outside surface of the sample holder) was subtracted at a steady-state condition at the corresponding RH before the uptake experiment as done in our previous work (Liu et al., 2015). The mean concentrations of SO_2, NO_2 and NH_3 were 8.3 ± 5.2 (0.4–49.1), 31.5 ± 13.2 (2.5–85.1) and 41.0 ± 18.4 (0.3–126.4) ppb, respectively, in polluted events (with the $PM_{2.5}$ concentration higher than 75 $\mu g\,m^{-3}$ and the RH less than 90 %) in Shijiazhuang. The initial concentrations of SO_2, NO_2 and NH_3 in the reactor were 190 ± 2.5, 100 ± 2.5 and 50 ± 2.5 ppb, respectively. The initial concentrations of NO_2 and NH_3 were close to their ambient concentrations, while a high initial SO_2 concentration was used here to obtain a good signal to noise ratio for γ_{SO_2} measurements. In this work, we aimed to understand the influence of AWC on the uptake kinetics of SO_2. Therefore, we fixed the initial concentrations of pollutants and the temperature at 300 K. SO_2 and NO_2 were measured using the corresponding analyzer (Thermo 43i and 42i), and NH_3 was measured by an ammonia analyzer (EAA-22, LGR, USA). The specific surface area of the mixture of A1 dust and NH_4NO_3 was 0.813 $m^2\,g^{-1}$, measured by a nitrogen BET physisorption analyzer (Quantachrome Autosorb-1-C). RH from 0 to 80 % was adjusted by varying the ratio of dry to wet zero air (water bubbler) and measured by a RH sensor (HMP110, Humicap). Control experiments demonstrate that adsorption of SO_2 on the quartz tube is negligible. It should be noted that the wall loss of SO_2 in the presence of NH_3 and/or NO_2 would be larger in the absence of seed aerosols. Additional control experiments in the presence of NO_2 and NH_3 demonstrate that the contribution of wall loss of SO_2 should be less than 3 % to the measured γ.

2.3 Calculations of AWC, aerosol pH and production rates of sulfate in aerosol liquid water

The AWC and aerosol pH in Shijiazhuang were calculated using the ISORROPIA II model using the measured concentrations of SO_4^{2-}, NH_4^+, NH_3, NO_3^-, HNO_3, Cl^-, HCl, Na^+, Ca^{2+}, K^+ and Mg^{2+}, as well as RH and temperature as input. The particles were assumed in metastable phase using a forward method (Song and Osada, 2020; Shi et al., 2019). The dataset with RH lower than 35 % was excluded (Pye et al., 2020) due to large uncertainties of aerosol pH (Ding et al., 2019; Guo et al., 2016; Pye et al., 2020). The pH was then calculated according to Pye et al. (2020) and Ding et al. (2019):

$$\mathrm{pH} = -\log_{10}(\gamma_{H^+} m_{H^+}) = -\log_{10}\frac{1000\gamma_{H^+} c_{H^+}}{\mathrm{AWC}}, \quad (3)$$

where γ_{H^+} is the activity coefficient of H^+, and m_{H^+} is the molality of H^+. The deliquescence curves of inorganic salts were calculated at 298.5 K using the E-AIM model (Clegg et al., 1998). Then, the AWC attributed to individual salt was calculated with the mass of the salt and the mass-based growth factor at the corresponding RH. The AWC of model particles for laboratory studies was also calculated with the known composition, while the aerosol pH values in Beijing were not calculated, because the concentrations of Na^+, Ca^{2+}, K^+ and Mg^{2+} were unavailable.

Similar to previous studies (P. Liu et al., 2020; Cheng et al., 2016), four oxidation pathways of S(IV) in aqueous-phase were accounted for, i.e., oxidation by O_3, H_2O_2, NO_2 and TMI (Fe^{3+} and Mn^{2+}), according to the following equations (Seinfeld and Pandis, 2006; Cheng et al., 2016; P. Liu et al., 2020):

$$-\left(\frac{\mathrm{d}[\mathrm{S(IV)}]}{\mathrm{d}t}\right)_{O_3} = \left(k_0\left[SO_{2,aq}\right] + k_1\left[HSO_3^-\right] + k_2\left[SO_3^{2-}\right]\right)\left[O_{3,aq}\right], \quad (4)$$

$$-\left(\frac{\mathrm{d}[\mathrm{S(IV)}]}{\mathrm{d}t}\right)_{H_2O_2} = \frac{k_3\left[H^+\right]\left[HSO_3^-\right]\left[H_2O_2,aq\right]}{1 + K\left[H^+\right]}, \quad (5)$$

$$-\left(\frac{\mathrm{d}[\mathrm{S(IV)}]}{\mathrm{d}t}\right)_{TMI} = k_4\left[H^+\right]^{\alpha}\left[Mn^{2+}\right]\left[Fe^{3+}\right][\mathrm{S(IV)}], \quad (6)$$

$$-\left(\frac{\mathrm{d}[\mathrm{S(IV)}]}{\mathrm{d}t}\right)_{NO_2} = k_5\left[NO_2,aq\right][\mathrm{S(IV)}], \quad (7)$$

where $k_0 = 2.4\times10^4\,M^{-1}\,s^{-1}$, $k_1 = 3.7\times10^5\,M^{-1}\,s^{-1}$, $k_2 = 1.5\times10^9\,M^{-1}\,s^{-1}$, $k_3 = 7.45\times10^7\,M^{-1}\,s^{-1}$, $K = 13\,M^{-1}$, $k_4 = 3.72\times10^7\,M^{-1}\,s^{-1}$, and $\alpha = -0.74$ (for $\mathrm{pH} \le 4.2$) or $k_4 = 2.51\times10^{13}\,M^{-1}\,s^{-1}$, $\alpha = 0.67$ (for $\mathrm{pH} > 4.2$), and $k_5 = (1.24\text{–}1.67)\times10^7\,M^{-1}\,s^{-1}$ (for $5.3 \le \mathrm{pH} \le 8.7$; the linear interpolated values were used for pH between 5.3 and 8.7) at 298 K (Clifton et al., 1988; P. Liu et al., 2020; Tilgner et al., 2021; Liu et al., 2021). [O_3, aq], [H_2O_2, aq] and [NO_2, aq] were calculated according to the Henry's constants, which are 1.1×10^{-2}, 1.0×10^5 and $1.2\times10^{-2}\,M\,atm^{-1}$ at 298 K for O_3, H_2O_2 and NO_2, respectively (Seinfeld and Pandis, 2006). H_2O_2 concentrations were unavailable during our observations. It was fitted based on temperature like in previous work (Fang et al., 2019). Figure S2 shows the derived H_2O_2 concentrations and the diurnal curves of H_2O_2 in winter in Shijiazhuang. The H_2O_2 concentrations varied from 0.05 to 3.7 ppbv, with a mean value of 0.62 ± 0.52 ppbv. Overall, the wintertime H_2O_2 concentrations derived in this work are comparable with those reported in the literature (Ye et al., 2018). The concentrations of Fe^{3+} and Mn^{2+} were calculated according to the measured total Fe and Mn concentrations assuming 18 % of total Fe and 30 % of total Mn were soluble (Wang et al., 2014; Cui et al., 2008) and the precipitation equilibriums of $Fe(OH)_3$ and $Mn(OH)_2$ depending on pH. The concentrations of Fe and Mn before December 2018 were estimated according to their mean ratios to $PM_{2.5}$ mass concentration (Wang et al., 2014), because the instrument was unavailable.

3 Results and discussion

3.1 Variation of sulfate in $PM_{2.5}$

Figure 1a shows the hourly mean mass concentration of $PM_{2.5}$ measured at SJZ and BUCT stations from 15 March 2018 to 15 April 2019. The mass concentration of $PM_{2.5}$ in Shijiazhuang generally coincided with that in Beijing. This highlights the regional characteristic of air pollution in BJH. However, Shijiazhuang usually showed significantly higher $PM_{2.5}$ concentration than that in Beijing. The hourly mean $PM_{2.5}$ concentration varied in the range of 0–650 $\mu g\,m^{-3}$ with an annual mean concentration of $86.4 \pm 77.8\,\mu g\,m^{-3}$. The corresponding values in Beijing were 1.5–556 and $55.0 \pm 51.0\,\mu g\,m^{-3}$. Particularly, the wintertime mass concentration of $PM_{2.5}$ in Shijiazhuang was around 2.4 times as that in Beijing. This is consistent with previous results that Shijiazhuang is suffering from more serious air pollution (D. Chen et al., 2019b) because of its larger density of heavy industries and more intensive emissions than in Beijing (D. Chen et al., 2019a).

Like the mass concentration of $PM_{2.5}$, both the mass concentration (Fig. 1b) and the fraction of sulfate in $PM_{2.5}$ (Fig. 1c) in Shijiazhuang were usually higher than those in Beijing. The annual mean sulfate concentrations in Shijiazhuang and Beijing were 11.7 ± 12.7 and $5.4 \pm 6.9\,\mu g\,m^{-3}$, which annually contributed 15.3 ± 8.7 % and 10.7 ± 7.3 % to the $PM_{2.5}$ mass concentrations, respectively. However, the molar ratio of NO_3^- to SO_4^{2-} (3.37 ± 3.05), corresponding to the mass ratio 2.17 ± 1.97 in Beijing was significantly higher than that in Shijiazhuang (2.69 ± 1.80, corresponding to mass ratio of 1.77 ± 1.72) at the 0.05 level. This is consistent with the emission inventories of air pollutants, in which Shijiazhuang had larger SO_2 emissions than Beijing, and vice versa for NO_x emissions (Yang et al., 2019; F. Liu et al., 2017; D. Chen et al., 2019a). A decrease of sulfate concentration ($5.4 \pm 6.9\,\mu g\,m^{-3}$) in Beijing was significant even when compared with that in $PM_{1.0}$ ($8.1 \pm 8.3\,\mu g\,m^{-3}$) measured from July 2011 to June 2012 (Sun et al., 2015), while the mass ratio of NO_3^-/SO_4^{2-} (2.17 ± 1.97) in Beijing showed an obvious increase compared with those in 2011–2012 (1.3–1.8) (Sun et al., 2015) and 2008 (0.8–1.5) (Zhang et al., 2013). This can be ascribed to the effective reduction of SO_2 emissions but less effective reduction of traffic emissions in Beijing.

The ground surface concentrations of pollutants are prone to be affected by variation of mixing layer height (MLH) (Zhong et al., 2018; Tang et al., 2016). Sulfur oxidation ratio (SOR), which is defined as the molar ratio of sulfate to total sulfur (Wang et al., 2005; Fang et al., 2019),

$$\mathrm{SOR} = \frac{n_{SO_4^{2-}}}{n_{SO_4^{2-}} + n_{SO_2}}, \quad (8)$$

was calculated and should be less affected by the MLH variation. As shown in Fig. 1e, the SOR in Beijing was overall higher than that in Shijiazhuang. Thus, the annual mean SOR in Beijing (0.42 ± 0.29) was comparable with that reported in literature (Fang et al., 2019), while it was significantly higher than that in Shijiazhuang (0.31 ± 0.19) at the 0.05 level. The high primary emissions of SO_2 in Shijiazhuang should lead to a lower SOR than that in Beijing. On the other hand, secondary transformation of SO_2 to sulfate should also have an influence on the SOR. The O_x ($O_x = NO_2 + O_3$) concentration in Shijiazhuang was usually higher than that in Beijing (Fig. 1f). The annual mean O_x concentration in Shijiazhuang was 55.2 ± 22.3 ppb, which was significantly higher than that in Beijing (50.7 ± 21.5 ppb) at the 0.05 level. This is inconsistent with the observed higher SOR in Beijing if gas-phase oxidation mainly contributed to sulfate formation. These results suggest that heterogeneous and/or multiphase reactions may also play important roles in particulate sulfate formation during transport (Zheng et al., 2015; Martin and Good, 1991; Wu et al., 2019).

Figure 2a–c show the mass concentration of $PM_{2.5}$ colored according to the mass concentration of sulfate, the fraction of sulfate in the soluble PM and the SOR in Shijiazhuang. In most serve pollution events, high $PM_{2.5}$ mass concentration coincided with the high sulfate concentration, the fraction of sulfate and the SOR (colored in grey color). For example, the mean $PM_{2.5}$ concentration was $411.7 \pm 98.1\,\mu g\,m^{-3}$ during the pollution event that occurred from 08:00 on 12 January 2019 to 00:00 on 15 January 2019 (All times in this paper are given in local time unless stated otherwise.). The corresponding sulfate concentration, fraction of sulfate in soluble PM and SOR were $80.6 \pm 24.0\,\mu g\,m^{-3}$, 39.4 ± 3.6 % and 0.79 ± 0.09, respectively. Other pollution episodes, which were highlighted in grey color in Fig. 2, showed a similar trend. The variations of the sulfate concentration, the fraction of sulfate in nonrefractory $PM_{2.5}$ and the SOR with $PM_{2.5}$ mass concentration in Beijing were similar to Shijiazhuang and shown in Fig. S3. These results confirm that the conversion rate of SO_2 to sulfate is promoted in pollution days when compared with that in clean days.

3.2 Role of aerosol water content in sulfate formation

Previous studies have found that severe pollution events are frequently accompanied with high RH (Zhang et al., 2018; Tang et al., 2016; Wu et al., 2018; Y. Liu et al., 2019; Clifton et al., 1988; Maahs, 1983; Martin and Good, 1991). As shown in Fig. 2d, the high concentration of sulfate positively correlated with high RH in most cases, which are shaded in grey columns. However, some pollution events (shaded in purple columns) also occurred under high RH, but the sulfate concentration or sulfate fraction in soluble PM was not so high. This means that high RH is a necessary but not a sufficient condition for sulfate conversion in severe haze pollution events. Thus, it is difficult to fully understand the general regularity behind the dataset or overemphasize the importance of a specific process in the atmosphere based on

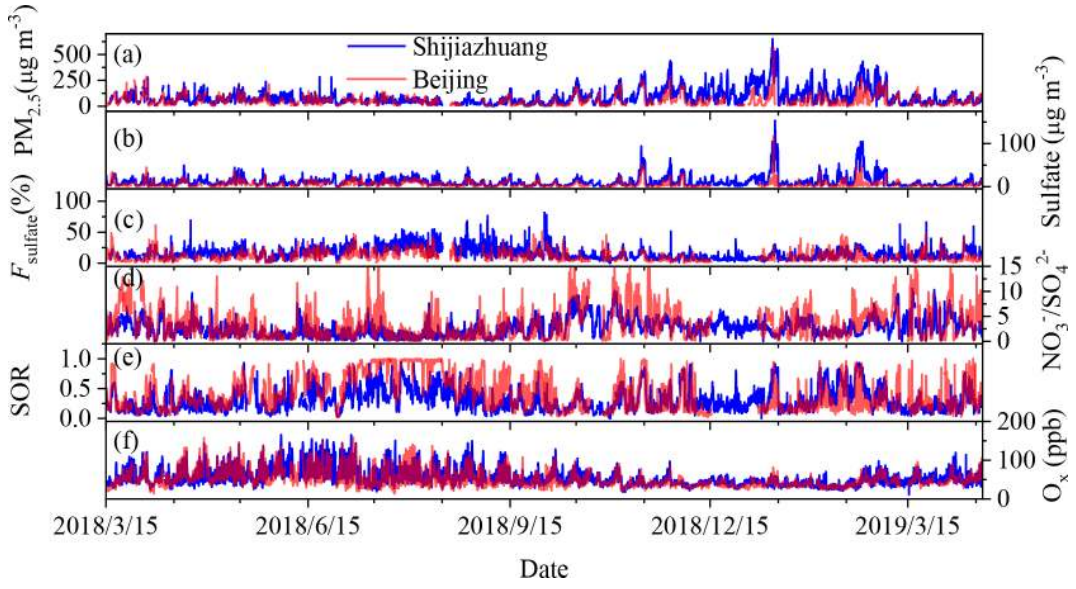

Figure 1. The hourly mean **(a)** mass concentration of $PM_{2.5}$, **(b)** sulfate concentration, **(c)** sulfate fraction in $PM_{2.5}$, **(d)** molar ratio of nitrate to sulfate, **(e)** sulfur oxidation ratio (SOR) and **(e)** O_x ($=NO_2+O_3$) concentration in Shijiazhuang and Beijing from 15 March 2018 to 15 April 2019.

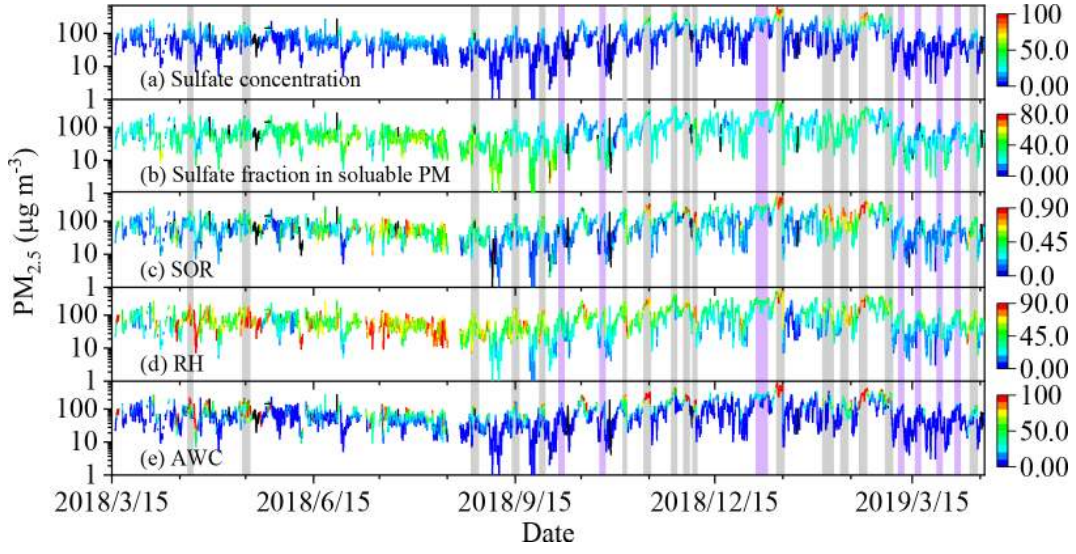

Figure 2. Mass concentration of $PM_{2.5}$ colored according to **(a)** sulfate concentration, **(b)** sulfate fraction in soluble PM, **(c)** SOR, **(d)** RH and **(e)** AWC in Shijiazhuang. The shade areas in grey indicate the pollution events with high concentration of sulfate at high RH, while the purple ones the mean pollution events with low sulfate fraction at high RH.

case studies. This might be the reason why contrary conclusions about the formation path of sulfate were drawn by different researchers. We statistically analyzed the relationship between the SOR and the RH. All the hourly mean data of the SOR and RH have been binned into 100×100 boxes. Then, the density of data points, which statistically indicates the occurrence of the events at given values of RH and SOR, was calculated using a bivariate kernel density estimator (Wand and Jones, 1993).

Figure 3a and b show the 2D kernel density graphs between the SOR and the RH in Shijiazhuang and Beijing. The color bar shows the density of data points. Although the SOR varied obviously at a certain RH, the most probable distribution of SOR could be exponentially fitted as a function of RH in Shijiazhuang (Fig. 3a); i.e., $\mathrm{SOR} = 0.15 + 0.0032 \times \exp(\mathrm{RH}/16.2)$ ($R = 0.79$). This is consistent with the dependence of SOR on RH based on previous studies (Tian et al., 2019; Wu et al., 2019). It should be noted that both SOR and

RH showed obvious diurnal variation (Fig. S4). Their diurnal variations were somewhat similar, but a 4 h time lag was observed between their minimum values. This means that the diurnal variations of SOR and RH might also contribute to the strong dependency of SOR on RH (Fig. 3a and b). However, the exponential dependency of SOR on RH was still observable in the night or in the day (Fig. S5a and b). It did so in winter or summer (Fig. S5c and d). This means that aqueous reactions are important for sulfate formation even if the influence of diurnal and seasonal variations are ruled out (Wang et al., 2016; Cheng et al., 2016).

In Fig. 3a, 72.5 % of the data points of Shijiazhuang (6509 over 8980 effective points) were in the domain with the RH range of 10 %–70 % and the SOR range of 0.05–0.42, while 10.1 % of data points were in the region with the RH greater than 70 % and the SOR greater than 0.42. The first region corresponded to a lower mean $PM_{2.5}$ concentration, sulfate concentration and SOR ($76.1 \pm 62.78\,\mu g\,m^{-3}$, of $8.1 \pm 6.3\,\mu g\,m^{-3}$, and 0.21 ± 0.09, respectively) compared with the second one ($115.7 \pm 96.7\,\mu g\,m^{-3}$, $22.4 \pm 20.4\,\mu g\,m^{-3}$ and 0.62 ± 0.14, respectively). As shown in Fig. 3b, the SOR also exponentially increased as a function of RH in Beijing. A percentage of 74.6 % of 8169 data points were in the first region. The mean $PM_{2.5}$ concentration, sulfate concentration and SOR were $48.2 \pm 44.8\,\mu g\,m^{-3}$, $2.9 \pm 3.0\,\mu g\,m^{-3}$ and 0.21 ± 0.10, respectively, in the low RH region, while they were $69.9 \pm 50.9\,\mu g\,m^{-3}$, $9.4 \pm 8.5\,\mu g\,m^{-3}$ and 0.83 ± 0.15 in the high RH region. The most probable distribution of SOR in Beijing could also be exponentially fitted as a function of RH ($SOR = -0.045 + 0.12 \times \exp(RH/37.8)$, $R = 0.92$). However, the SOR was more sensitive to RH in Beijing than that in Shijiazhuang. This might be explained by the increased importance of sulfate formation via gas-phase reactions in Beijing (Fang et al., 2019; Hollaway et al., 2019), because the $PM_{2.5}$ mass concentrations in Beijing were significantly lower than that in Shijiazhuang (Fig. 1).

Formation of particle-phase sulfate through heterogeneous or multiphase oxidations includes the uptake of SO_2 and the following oxidation in particle phase. Thus, it is meaningful to identify the rate-determining step (RDS) for understanding the evolution of the SOR. As shown in Fig. 3, the initial $\gamma_{SO_2,BET}$ increased exponentially from 0 to $(1.13 \pm 0.21) \times 10^{-5}$ when the RH increases from 2 % to 80 % in the presence of 50 ± 2.5 ppb NH_3 with or without 100 ± 2.5 ppb NO_2. The dependence of $\gamma_{SO_2,BET}$ on RH was $\gamma_{SO_2,BET} = 2.44E-7+6.69E-8 \times \exp(RH/17.4)$ with a correlation coefficient of 0.96. A transition region of the $\gamma_{SO_2,BET}$ versus the RH was observable when the RH ranged from 60 % to 80 %. When the RH was higher than 70 %, the $\gamma_{SO_2,BET}$ increased quickly as a function of the RH. The similar dependency on RH for the $\gamma_{SO_2,BET}$ and the SOR suggests that the uptake kinetic of SO_2 might determine sulfate formation.

In a previous work (Zhang et al., 2019), it has been found that all the uptake of SO_2 on dust or nitrate-coated dust can be transformed into sulfate over the timescale of the uptake experiment using the similar coated-wall flow tube reactor. Another study also observed a quick formation of sulfate on the surface of aqueous microdroplets under acidic conditions (pH < 3.5) without the addition of other oxidants, which was explained by the direct interfacial electron transfer from SO_2 to O_2 on the aqueous microdroplets (Hung et al., 2018). The pH of deliquesced NH_4NO_3 is 4.2 as calculated using the ISORROPIA II model. This means that oxidation of S(IV) might not be a RDS of sulfate formation. The oxidation processes can be ascribed to catalytic oxidation by O_2 in the presence of transition metals, oxidation by O_2 and nitric acid promoted by protons in the presence of nitrate (Zhang et al., 2019) and the oxidation by other dissolved oxidants in liquid phase (T. Chen et al., 2019; Cheng et al., 2016; Wang et al., 2016). To further validate this assumption, the formation rates of SO_4^{2-} ($d[SO_4^{2-}]/dt$) in aerosol liquid phase were calculated according to the method used in previous work (P. Liu et al., 2020; Cheng et al., 2016). If oxidation of S(IV) is the rate-determining step, the formation rate should show a similar dependence on RH like the SOR.

As shown in Fig. 4a, the relative contributions of different oxidation paths of S(IV) varied obviously case by case. In summer and autumn, oxidation by H_2O_2 was the most important path followed by TMI. In winter, however, NO_2, O_3 or H_2O_2 could contribute to the major oxidation path. This might be the reason why these oxidation paths showed inconsistent relative importance of among different studies even using the same method, such as isotopic measurements (Shao et al., 2019; He et al., 2018). Figure 4b and c show the dependence of the formation rates of sulfate on RH in the range of 35 %–100 % in Shijiazhuang. The dataset for RH below 35 % was omitted due to the large uncertainty in aerosol pH calculations (Ding et al., 2019; Guo et al., 2016; Pye et al., 2020). The relative contributions of different oxidation paths of S(IV) also varied obviously as a function of RH. NO_2 and O_3 played important role in aqueous S(IV) oxidation when RH was from 35 % to 45 %, while TMI became the dominator when RH ranged from 45 % to 70 %. Above 70 % RH, the contribution of H_2O_2 was dominant, which is consistent with several recent studies (P. Liu et al., 2020; T. Liu et al., 2020). However, the total formation rate of sulfate in aerosol liquid phase slightly decreased as RH increased. A weak downward trend of the $d[SO_4^{2-}]/dt$ rate with RH was also observable in the 2D kernel density graphs as shown in Fig. 4c. This is opposite to the dependencies of the SOR and the γ_{SO_2} on RH as discussed above, which means the RDS for sulfate formation should be the uptake of SO_2 instead of oxidation of S(IV) in aqueous phase. We further calculated the production rate of sulfate through uptake of SO_2 (mass transfer to aerosol

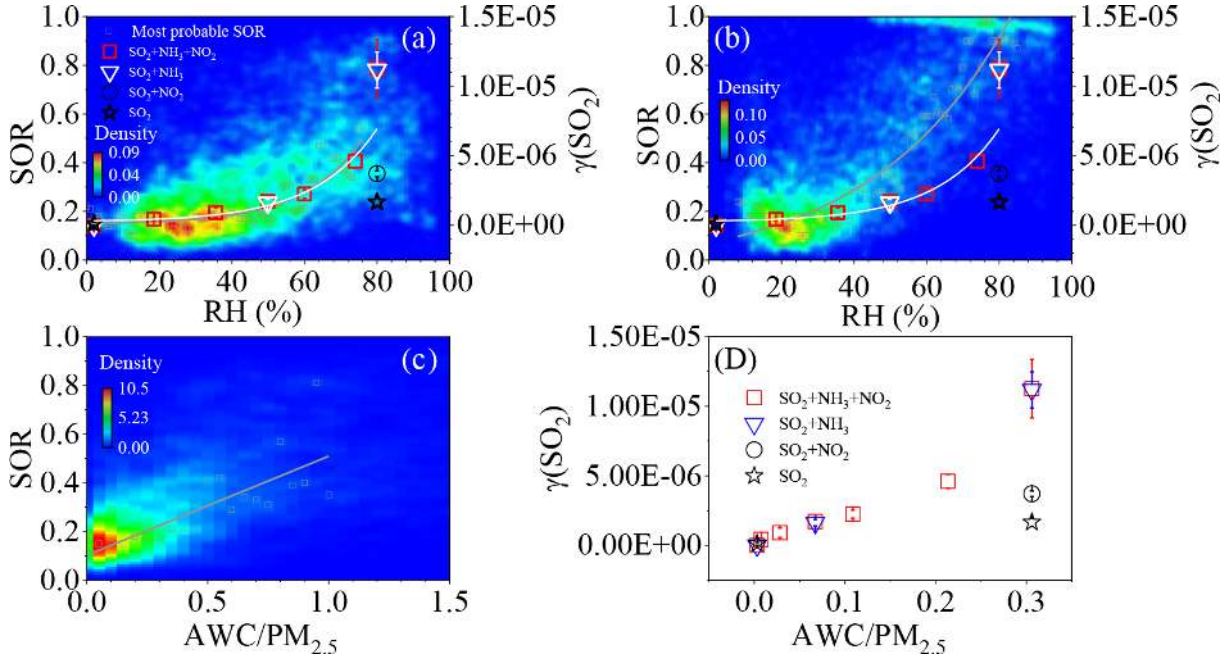

Figure 3. Relationship between SOR and $\gamma_{SO_2,BET}$ on dust internally mixed with NH_4NO_3 (2 : 1) and RH in **(a)** Shijiazhuang and **(b)** Beijing and the correlation of **(c)** SOR in Shijiazhuang and **(d)** $\gamma_{SO_2,BET}$ with $AWC/PM_{2.5}$. The initial concentrations of SO_2, NO_2 and/or NH_3 in the flow tube reactor were 190 ± 2.5, 100 ± 2.5 and/or 50 ± 2.5 ppb, respectively. The grey lines are the fitting curves for the most probable SOR, and the white lines are the fitting curves for the $\gamma_{SO_2,BET}$.

particles) according to

$$\frac{d\left[SO_4^{2-}\right]}{dt} = 3600 \cdot \frac{96}{64} \cdot \frac{\gamma_{SO_2} A_s \omega c_{SO_2}}{4}, \quad (9)$$

where A_s is the surface area concentration of $PM_{2.5}$, ω is the mean molecular velocity of SO_2 and c_{SO_2} is the mass concentration of SO_2. As shown in Fig. 4c, the probability-weighted production rate of sulfate through uptake of SO_2 (the grey line) is lower than that through aqueous oxidation of S(IV), in particular, when RH is lower than 70 %. It should be noted that the mass transfer of SO_2 was not assumed to be the RDS using a large mass accommodation coefficient of SO_2 ($\alpha = 0.11$) (Cheng et al., 2016). According to the relationship between the mass accommodation coefficient (α) and the uptake coefficient (γ) of SO_2 (Kulmala and Wagner, 2001), the α_{SO_2} on particles is on the same order of the γ_{SO_2}. This means that mass transfer rate might have been overestimated by Cheng et al. (2016).

Phase state is a crucial factor determining the mass transfer of pollutants from gas phase to particle phase (Davis et al., 2015; Marshall et al., 2018; Shiraiwa et al., 2011; Liu et al., 2014), while the AWC or RH greatly affects the phase state of aerosol particles (Duan et al., 2019; Y. Liu et al., 2019; Shiraiwa et al., 2017). For example, ambient particles were found to change from semisolid to liquid state when the RH was above ~ 60 % (Y. Liu et al., 2019, 2017), corresponding to the AWC higher than ~ 15 $\mu g\, m^{-3}$ (Y. Liu et al., 2017) under the typical urban environment in Beijing based on rebound fractions measurements. It was also confirmed that haze particles displayed a solid–aqueous equilibrium state when the RH was around 60 %–80 % using an individual particle hygroscopicity system (Sun et al., 2018). As shown in Fig. S6, the most probable distribution of the AWC exponentially increased with the RH ($AWC = -5.76 + 5.15 \times \exp(RH/36.1)$, $R = 0.98$) in Shijiazhuang. An obvious transition region of the RH between 60 % and 80 % was also observed. These results indicate that the liquid-phase aerosol should appear when the RH is higher than ~ 60 % (Y. Liu et al., 2019, 2017) and subsequently promote the conversion of SO_2 to sulfate. The SOR increased as a power function of AWC ($SOR = 0.072 + 0.043 \times AWC^{0.53}$, $R = 0.78$), while it was linearly correlated with the ratio of $AWC/PM_{2.5}$ ($SOR = 0.15 + 0.40 \times AWC/PM_{2.5}$, $R = 0.78$) as shown in Fig. 3c. Similarly, the AWC of dust internally mixed with NH_4NO_3 was also calculated using the ISORROPIA II model. The $\gamma_{SO_2,BET}$ also showed a similar trend as a function of $AWC/PM_{2.5}$ ($\gamma_{SO_2,BET} = 3.08E-5 \times AWC/PM_{2.5}$, $R = 0.95$) (Fig. 3d), although the ranges of $AWC/PM_{2.5}$ were different due to the difference in aerosol composition. This means that the fraction of aerosol liquid water governs both the conversion of SO_2 to sulfate and uptake kinetics of SO_2.

It should be noted that although the SOR showed a similar RH dependence as the SO_2, a deviation was observed in both Shijiazhuang and Beijing (Fig. 3). The γ_{SO_2} was mea-

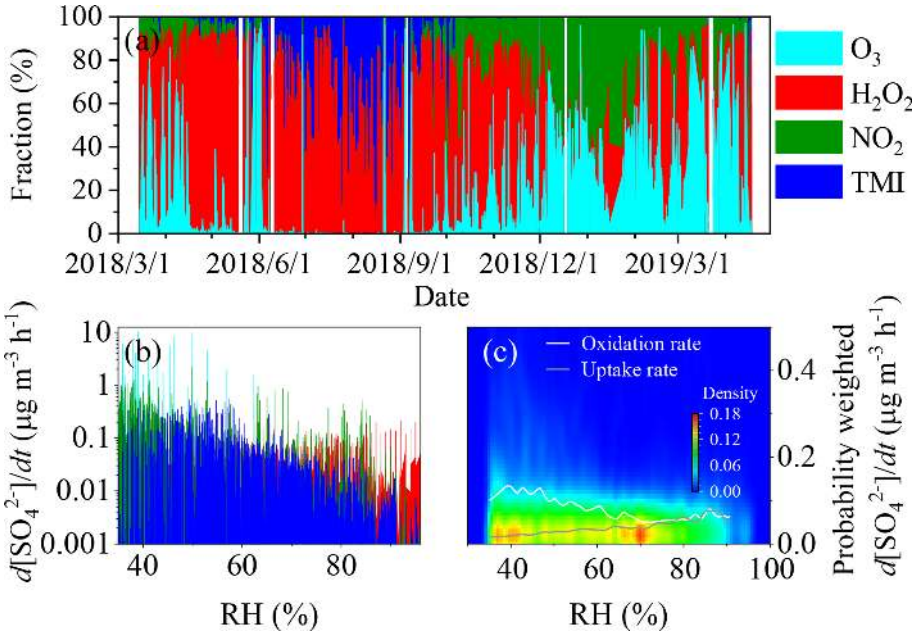

Figure 4. **(a)** The relative importance of oxidation paths of S(IV) in aqueous phase, the dependence of **(b)** sulfate formation rates and **(c)** the probability-weighted sulfate formation rates on RH in Shijiazhuang.

sured at a fixed temperature and initial SO_2 concentration. In the atmosphere, both of them varied obviously. This might lead to the observed deviation. On the other hand, the coexisted components such as organic aerosol and black carbon in atmospheric particles should have complicated the influence on the hygroscopicity and the phase change of particles. The difference between the model particles and the real ambient aerosol particles might also partially lead to the deviations of the RH dependence between the SOR and the $\gamma_{SO_2,BET}$. In addition, it also implies that besides the reaction in aerosol liquid phase, other reaction paths such as oxidation of SO_2 by gas-phase oxidants should also play an important role in sulfate formation (Duan et al., 2019).

3.3 Influence of particle composition on AWC and sulfate formation

Besides RH, particle composition is another important factor to affect the AWC. According to the ions balance (Fig. S7a), ammonia was adequate to neutralize the anions in $PM_{2.5}$, which is consistent with the results in the literature (Y. Wang et al., 2020b). In addition, (81.5 ± 15.9) % (with the median of 87.1 %) of ionic anions (nitrate, chloride and sulfate) were neutralized by ammonium (Fig. S7b). This means NH_4NO_3, $(NH_4)_2SO_4$ and NH_4Cl should be the dominant form of nitrate, sulfate and chloride in $PM_{2.5}$, respectively. We further reconstructed the molecular composition from the ions based on the principles of aerosol neutralization and molecular thermodynamics (Kortelainen et al., 2017). The molecular concentrations were estimated according to the molar ratio of NH_4^+ to SO_4^{2-} ($R_{NH_4+/SO_4^{2-}}$) according to the following rules: (i) if $0<R_{NH_4+/SO_4^{2-}}<1$, NH_4^+ existed as the chemical forms of H_2SO_4 and NH_4HSO_4; (ii) $1<R_{NH_4+/SO_4^{2-}}<2$, NH_4^+ existed as $(NH_4)_2SO_4$ and NH_4HSO_4; (iii) if $R_{NH_4+/SO_4^{2-}}>2$, then the fraction NH_4^+ corresponding to twice the amount of SO_4^{2-} existed as $(NH_4)_2SO_4$, and the remaining fraction of NH_4^+ was associated with NO_3^- and Cl^-; and (iv) the rest of NO_3^-, which was not neutralized by NH_4^+, was from $NaNO_3$. Figure 5a and b show the variation of the molecular composition as a function of RH in Shijiazhuang. Obviously, NH_4NO_3 and $(NH_4)_2SO_4$ were the major molecular components. Both of them showed upward trend as the RH increased. In particular, the fraction of NH_4NO_3 increased gradually from $\sim$ 10 % to $\sim$ 50 % when the RH increased from $\sim$ 30 % to 90 %. Correspondingly, the fraction of $(NH_4)_2SO_4$ decreased as the RH increased.

It should be noted that the deliquescence RH (DRH) of NH_4NO_3 (61.8 %) (Onasch et al., 1999) is lower than those values of NH_4Cl (78 %) (Hu et al., 2011) and $(NH_4)_2SO_4$ (80 %) (Lightstone et al., 2000). We further calculated the AWC attributed to the individual molecular component based on the growth factors and mass concentrations. As shown in Fig. 5c, the sum of the AWC of individual salts is underestimated by around 13 % compared to that calculated using the ISORROPIA II model (the grey line), because the mixing state was not considered in the former method. However, we can still draw a conclusion that NH_4NO_3 and $(NH_4)_2SO_4$ are the major contributors to the AWC. Especially NH_4NO_3

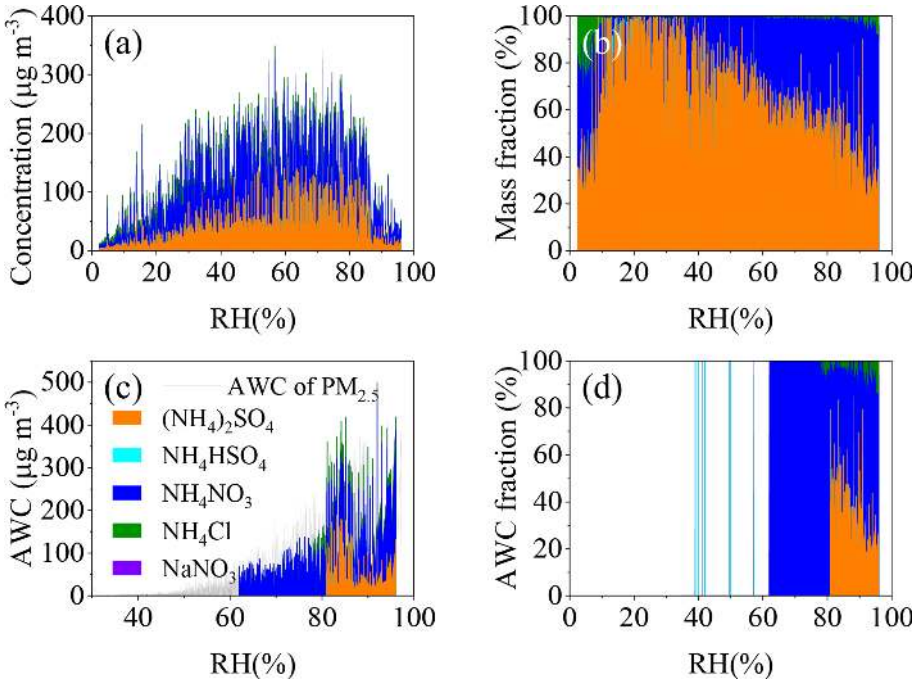

Figure 5. Variations of **(a)** the mass concentrations and **(b)** the mass fractions of molecular composition in $PM_{2.5}$, **(c)** the estimated AWC attributed to different composition and **(d)** the corresponding AWC fraction as a function of RH in Shijiazhuang.

dominated the AWC when the RH ranged from 60 % to 80 %, in which the SOR and the γ_{SO_2} were very sensitive to RH. These results suggest that NH_4NO_3 should be the most important mediator to AWC and subsequently the uptake of SO_2 in the transition regime of RH in Fig. 3a. It should be noted that $(NH_4)HSO_4$ has a lower DRH than NH_4NO_3 (Y. J. Li et al., 2017). However, 98.4 % of the data points showed an $R_{NH_4^+/SO_4^{2-}}$ higher than 2.0 in Shijiazhuang. This means that the contribution of $(NH_4)HSO_4$ to $PM_{2.5}$ should be negligible because of the abundance of atmospheric NH_3 in northern China. In previous work, it has been found that SO_2 oxidation can be promoted by particulate nitrate through the accumulation of proton (Zhang et al., 2019) and the formation of $NO^+NO_3^-$ (Kong et al., 2014). Our results further showed the importance of NH_4NO_3 in the AWC, which possibly determines the phase state of particles and subsequently the uptake kinetics of SO_2 and the SOR as discussed above. To further confirm the role of NH_4NO_3 in the uptake of SO_2, uptake experiment of SO_2 on pure dust has been carried out at 2 % and 80 % RH. The corresponding $\gamma_{SO_2,BET}$ was $1.10 \pm 1.05 \times 10^{-7}$ and $1.66 \pm 0.28 \times 10^{-7}$ on pure dust sample in the presence of NH_3 and NO_2. However, as discussed above, it was 0 and $1.12 \pm 0.15 \times 10^{-5}$ on dust internally mixed with 33 % NH_4NO_3. This directly confirmed the role of NH_4NO_3 in SO_2 uptake via aerosol liquid water.

Figure S8 shows the dependencies of the $AWC/PM_{2.5}$ and SOR on the fraction of the individual molecular component. Both the $AWC/PM_{2.5}$ and SOR statistically increased as the fraction of NH_4NO_3 increased (Fig. S8a and d). A weak increase followed by a decrease was observed for the $AWC/PM_{2.5}$ as the fraction of $(NH_4)_2SO_4$ increased, while a negative correlation between the $AWC/PM_{2.5}$ and the fraction of NH_4Cl was observed. It did so for the SOR and the fraction of NH_4Cl. These phenomena were overall consistent with the sequence of their hygroscopicity. In addition, chloride is a primary pollutant mainly from coal combustion and biomass burning (Bi et al., 2019). Besides chloride, other primary particles from combustion such as soot, which were not accounted for in this work, might also decrease the uptake capability of water and subsequently be unfavorable for SO_2 uptake.

To assess the relative importance of sulfate and nitrate (the major SIA component) to AWC, the sensitivity of their fraction to AWC in Shijiazhuang was tested using the ISORROPIA II model and shown in Fig. S9. The base case means the AWC was calculated using the measured concentration of the ions. Then, we reduced the fraction of NH_4NO_3 or $(NH_4)_2SO_4$ from 0 to 80 % individually compared with the base case. Figure S9a shows the time series of the calculated AWC after reducing 50 % of NH_4NO_3 or $(NH_4)_2SO_4$. Reduction of either NH_4NO_3 or $(NH_4)_2SO_4$ resulted into obvious decrease of AWC during pollution events. In most cases, the reduction amplitude of AWC was larger when reducing 50 % of NH_4NO_3 than $(NH_4)_2SO_4$. Figure S9b shows the mean ratio of AWC at a certain reduction fraction of NH_4NO_3 or $(NH_4)_2SO_4$ to that under the base case. When NH_4NO_3 was reduced from 0 % to 80 %, the AWC linearly reduced from 0 % to 61.1 ± 0.1 % with a slope of 0.48 %.

It varied from 0 % to 66.0 ± 0.2 % for $(NH_4)_2SO_4$ (with a slope of 0.41 %). This means that the AWC is more sensitive to the fraction of NH_4NO_3 than $(NH_4)_2SO_4$ in Shijiazhuang. This also implies the importance of NH_4NO_3 in the observed high AWC in haze days. On the other hand, reducing 10 % of NH_4NO_3 can lead to a reduction of 5.2 ± 1.0 % AWC during haze days. Subsequently, we can roughly estimate that the SOR might be reduced by ∼ 4 % through a linear interpolation according to the equation of the SOR and the AWC/$PM_{2.5}$ (SOR = 0.15 + 0.40 × AWC/$PM_{2.5}$) fitted in Fig. 3c. This means reduction of NO_x and NH_3 should lead to additional reduction of particulate sulfate.

3.4 Influence of other factors on sulfate formation

Several studies have proposed out that NO_2 can promote the oxidation of SO_2 on particle surfaces and in aqueous phase. For example, laboratory studies have found that parts per million (ppm) levels of NO_2 can promote sulfate formation on the surface of dust through $NO^+NO_3^-$ which is disproportionated from N_2O_4 intermediate (He et al., 2014; Liu et al., 2012; Ma et al., 2008) or parts per million levels of NO_2 can promote the oxidation of SO_2 in the deliquesced oxalic acid (Wang et al., 2016). This is supported by the evidence that a high fraction of sulfate in $PM_{2.5}$ is positively correlated with NO_2 concentration (Xie et al., 2015) and that a high $PM_{2.5}$ concentration is accompanied with high ratio of NO_2/SO_2 in several case studies (He et al., 2014). The importance of the SO_2 oxidation by NO_2 in aqueous phase has also been confirmed in modeling studies (Cheng et al., 2016; Xue et al., 2016). However, this reaction path is still under debate because of the following reasons. (1) The concentration of NO_2 in laboratory studies was about 2 orders of magnitude higher than that in ambient air. This will affect the surface concentration of the intermediate (N_2O_4) and the concentration of solved NO_2 in aqueous phase. (2) The dissolved NO_2 concentration is highly sensitive to pH. The pH value in aerosol was 5.6–6.2 estimated in modeling study (Cheng et al., 2016). However, a recent work found that it varied from 3.8 to 4.5 at RH > 30 % and showed a moderate acidity because of the thermodynamic equilibrium between NH_4^+ and NH_3 (Ding et al., 2019). (3) The previous calculations were conducted using a high reaction rate constant of the NO_2 reaction with dissolved S(IV) (Clifton et al., 1988; Cheng et al., 2016), while a smaller value was reported in the more recent study (Spindler et al., 2003; Tilgner et al., 2021). (4) The relative importance of each path depends on the concentration of the relevant pollutants including H_2O_2 and TMI (P. Liu et al., 2020). Therefore, it is necessary to verify the importance of this process by long-term observation at different environments.

Figure 6 shows the 2D kernel density graph of the sulfate fraction in soluble PM and the SOR in Shijiazhuang as a function of the concentration of different gas-phase pollutants. It should be pointed out that the SOR or the γ_{SO_2} should be positively correlated to NO_2 concentration if it can promote the conversion of SO_2 to sulfate or the uptake of SO_2. However, both sulfate fraction and SOR were negatively correlated with the concentration of NO_2 from the point of view of statistics. A same trend was observed in Beijing (Fig. S10). This is similar to recent studies that observed the opposite correlation between SOR and NO_x concentration in the Sichuan Basin (Tian et al., 2019) and in Beijing (Fang et al., 2019). This means that NO_2 concentration is statistically not a determining factor for sulfate formation in the atmosphere. This is well supported by the uptake kinetics of SO_2 measured using a flow tube reactor. As shown in Fig. 3a and b, when 50 ± 2.5 ppb of NH_3 presenting in the reactant gases, no difference was observable for the $\gamma_{SO_2,BET}$ between the presence (red squares) and absence of 100 ± 2.5 ppb of NO_2 (white triangles). This is consistent with these previous studies that found NO_2 to be having no influence on SO_2 uptake when NH_3 was abundant in the atmosphere (Wu et al., 2019; Wang et al., 2021). In addition, it is consistent with the fact that H_2O_2 dominated the oxidation of S(IV) in aerosol liquid water when RH was higher than 60 % (Fig. 4a). It should be pointed out that the γ_{SO_2} at 80 % RH was $1.7 \pm 0.3 \times 10^{-6}$ on the mixture of dust and NH_4NO_3 in the absence of NH_3 and NO_2 (Fig. 3). It increased to $3.7 \pm 0.2 \times 10^{-6}$ in the presence of NO_2. This is consistent with the promotion effect of NO_2 for converting SO_2 to sulfate in the absence of NH_3 as observed in both a smog chamber (Wang et al., 2016) and a bubbling reactor (T. Chen et al., 2019). However, the enhanced uptake of SO_2 induced by NO_2 might be too low to be measured in the presence of NH_3. Therefore, the weak promotion effect by NO_2 alone cannot explain the negative correlation between the SOR and the concentration of NO_2 in Fig. 6f.

Both the fraction of sulfate and the SOR in Shijiazhuang statistically decreased as a function of SO_2 and CO concentration, respectively (Fig. 6b, c, g and h). This might be explained by the high concentration of primary aerosol components when pollution events occurred with high concentrations of primary gas-phase pollutants. However, the fraction of sulfate increased as a function of O_3 (Fig. 6d). When the O_3 concentration was greater than 50 ppb, the SOR slightly increased with the O_3 concentration (Fig. 6i). A more obvious positive dependence of sulfate fraction on O_3 concentration was observed in Beijing (Fig. S10e). This means oxidation capacity also plays an important role in sulfate formation, especially in Beijing. This is consistent with the recent finding that O_3 plays an important role in SO_2 oxidation at different locations (Fang et al., 2019; Tian et al., 2019; Duan et al., 2019). As shown in Fig. 6j, the SOR positively correlated with the concentration of NH_3 in Shijiazhuang. This means that NH_3 can promote the conversion of SO_2 to sulfate. This is well in agreement with laboratory studies that observed the promotion effect by NH_3 to the heterogeneous reaction of SO_2 on different mineral oxides (Yang et al., 2016). In addition, flow tube experi-

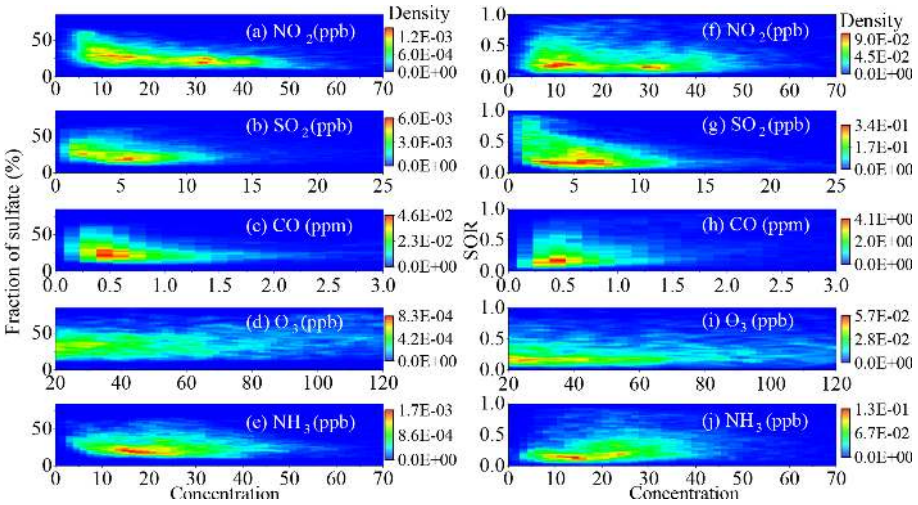

Figure 6. Dependence of the sulfate fraction in soluble PM and the SOR on gaseous pollutant concentration in Shijiazhuang.

ments were also carried out by exposing the internal mixing sample (2 : 1 dust and NH_4NO_3) to 200 ± 2.5 ppb SO_2 in the absence of NH_3 and NO_2 at 2 % and 80 % RH, respectively. As shown in Fig. 3a and b, the $\gamma_{SO_2,BET}$ was zero regardless of the reactants under dry condition (2 % RH), while it increased to $(1.66 \pm 0.28) \times 10^{-6}$ at 80 % RH. However, it was significantly smaller than the $\gamma_{SO_2,BET}$ ($(1.13 \pm 0.21) \times 10^{-5}$) in the presence of 50 ± 2.5 ppb NH_3 with or without 100 ± 2.5 ppb NO_2. These results further confirm that NH_3 can promote the uptake of SO_2 at high RH, possible through enhancing the solubility of SO_2 in water (T. Chen et al., 2019; Cheng et al., 2016; Wang et al., 2016), because the effective solubility of SO_2 can be enhanced due to the increase of the aerosol pH.

Aerosol acidity is one of the important factors affecting the sulfate formation and the partitioning of semivolatile gases in the atmosphere (Liu et al., 2021). As shown in Fig. S11, when aerosol pH is lower than 4.5, the oxidation rate of S(IV) in aerosol liquid phase decreases with decreasing pH, because the oxidation of S(IV) by transition metals is the dominant path and is decreasing with aerosol pH. However, the oxidation rate of S(IV) increases when the aerosol pH is higher than 4.5. This can be explained by the fact that the solubility and effective Henry's law constant of SO_2 are positively dependent on pH (Cheng et al., 2016; Liu et al., 2021; P. Liu et al., 2020), which is consistent with the promotion effect of sulfate formation by NH_3.

4 Conclusions and atmospheric implications

Based on 1 year of observations, we confirmed that high $PM_{2.5}$ mass concentration in pollution events usually coincided with the high sulfate concentration, the fraction of sulfate, and the SOR in both Beijing and Shijiazhuang. In Shijiazhuang, the SOR exponentially increased as a function of RH from the point of view of statistics, which was similar to the RH dependence of the γ_{SO_2} on the model particles containing 33 % NH_4NO_3 in the presence of NH_3. The SOR and γ_{SO_2} linearly increased as a function of the fraction of aerosol water content in $PM_{2.5}$. The enhanced uptake coefficient of SO_2 at high RH after the liquid-phase aerosol appeared might explain the increased SOR, because uptake of SO_2 was the rate-determining step for the conversion of SO_2 to particulate sulfate. NH_4NO_3 played an important role in the AWC, the phase state of aerosol particles and subsequently the uptake kinetics of SO_2 in haze days under high RH conditions.

The contribution of nitrate to $PM_{2.5}$ is increasing in China (Li et al., 2018; Tian et al., 2019) due to the intensive emissions of NO_x from steel production and cement manufacturing (Wu et al., 2018; Qi et al., 2017) as well as the increasing NO_x emissions from traffic (Liu et al., 2007; Wang et al., 2011). The mean fraction of nitrate in $PM_{2.5}$ was 21.4 ± 12.4 % in Shijiazhuang and 15.8 ± 13.4 % in Beijing. They were close to the reported values in $PM_{1.0}$ during the summer of Beijing (24 %) (Li et al., 2018) and in $PM_{2.5}$ during the winter of Chengdu (23.3 %) and Chongqing (17.5 %) (Tian et al., 2019). It has been found that the fraction of nitrate and ammonium usually increases as a function of $PM_{2.5}$ mass concentration (Li et al., 2018). Therefore, NO_x should be an urgent air pollutant in the future in China even from the point view of its contribution to $PM_{2.5}$ mass.

As observed in this work, NH_4NO_3 has an important contribution to $PM_{2.5}$ mass concentration, the aerosol water content and subsequently the phase state of particles in the RH range of 60 %–80 %. Reduction of NO_x emissions should lead to a decrease in NH_4NO_3 concentration and subsequently the AWC during serve pollution events. This will lead to an additional reduction of SO_2 uptake and the formation of particulate sulfate through aqueous reactions. Based on our rough estimation, 4 % of sulfate might be reduced due

to aqueous reaction in Shijiazhuang if the mass concentration of NH_4NO_3 was reduced by 10 %. More work is required to quantitatively assess the contribution of nitrate to sulfate formation from aqueous reactions in the future. It should be noted that ozone pollution becomes more and more important in China (Z. Chen et al., 2019; Ziemke et al., 2019). This requires us to harmoniously reduce NO_x and volatile organic compounds in the near future. It is also important to take actions on NH_3 emission control in the future as NH_3 can significantly promote the uptake of SO_2 in liquid-phase aerosol.

Data availability. The experimental data are available upon request to the corresponding authors.

Supplement. The supplement related to this article is available online at: https://doi.org/10.5194/acp-21-13269-2021-supplement.

Author contributions. YoL and XB designed the experiments. YoL and YuL wrote the paper. ZF, FZ, YZ, XF, CY, BC, YW, WD and JC carried out measurements at BUCT. XB and TJ carried out measurements at SJZ. YG, YZ and YoL carried out flow tube experiments. PL, YM and YoL performed sulfate formation calculations. YuL, FB, TP, YM, HH and MK revised the paper.

Competing interests. The authors declare that they have no conflict of interest.

Disclaimer. Publisher's note: Copernicus Publications remains neutral with regard to jurisdictional claims in published maps and institutional affiliations.

Acknowledgements. The research was financially supported by the National Natural Science Foundation of China (92044301), the Ministry of Science and Technology of the People's Republic of China (2019YFC0214701), Academy of Finland via the Center of Excellence in Atmospheric Sciences (272041, 316114, 315203 and 1307537), and European Research Council via ATM-GTP 266 (742206) and via ERA-NET-Cofund through SMart URBan Solutions for air quality, disasters and city growth (SMURBS/ERA-PLANET), the Strategic Priority Research Program of Chinese Academy of Sciences and Beijing University of Chemical Technology.

Financial support. This research has been supported by the National Natural Science Foundation of China (grant no. 92044301) and the Ministry of Science and Technology of the People's Republic of China (grant no. 2019YFC0214701), Academy of Finland via the Center of Excellence in Atmospheric Sciences (272041, 316114, 315203 and 1307537), and European Research Council via ATM-GTP 266 (742206) and via ERA-NET-Cofund through SMart URBan Solutions for air quality, disasters and city growth (SMURBS/ERA PLANET), the Strategic Priority Research Program of Chinese Academy of Sciences and Beijing University of Chemical Technology.

Review statement. This paper was edited by Harald Saathoff and reviewed by two anonymous referees.

References

An, Z., Huang, R.-J., Zhang, R., Tie, X., Li, G., Cao, J., Zhou, W., Shi, Z., Han, Y., Gu, Z., and Ji, Y.: Severe haze in northern China: A synergy of anthropogenic emissions and atmospheric processes, P. Natl. Acad. Sci. USA, 116, 8657–8666, https://doi.org/10.1073/pnas.1900125116, 2019.

Bi, X., Dai, Q., Wu, J., Zhang, Q., Zhang, W., Luo, R., Cheng, Y., Zhang, J., Wang, L., Yu, Z., Zhang, Y., Tian, Y., and Feng, Y.: Characteristics of the main primary source profiles of particulate matter across China from 1987 to 2017, Atmos. Chem. Phys., 19, 3223–3243, https://doi.org/10.5194/acp-19-3223-2019, 2019.

Chen, D., Liu, Z., Ban, J., and Chen, M.: The 2015 and 2016 wintertime air pollution in China: SO_2 emission changes derived from a WRF-Chem/EnKF coupled data assimilation system , Atmos. Chem. Phys., 19, 8619–8650, https://doi.org/10.5194/acp-19-8619-2019, 2019a.

Chen, D., Liu, Z., Ban, J., Zhao, P., and Chen, M.: Retrospective analysis of 2015–2017 wintertime $PM_{2.5}$ in China: response to emission regulations and the role of meteorology, Atmos. Chem. Phys., 19, 7409–7427, https://doi.org/10.5194/acp-19-7409-2019, 2019b.

Chen, Q., Sheng, L. F., Gao, Y., Miao, Y. C., Hai, S. F., Gao, S. H., and Gao, Y.: The Effects of the Trans-Regional Transport of $PM_{2.5}$ on a Heavy Haze Event in the Pearl River Delta in January 2015, Atmosphere, 10, 237, https://doi.org/10.3390/atmos10050237, 2019.

Chen, T., Chu, B., Ge, Y., Zhang, S., Ma, Q., He, H., and Li, S.-M.: Enhancement of aqueous sulfate formation by the coexistence of NO_2/NH_3 under high ionic strengths in aerosol water, Environ. Pollut., 252, 236–244, https://doi.org/10.1016/j.envpol.2019.05.119, 2019.

Chen, Z., Zhuang, Y., Xie, X., Chen, D., Cheng, N., Yang, L., and Li, R.: Understanding long-term variations of meteorological influences on ground ozone concentrations in Beijing During 2006–2016, Environ. Pollut., 245, 29–37, https://doi.org/10.1016/j.envpol.2018.10.117, 2019.

Cheng, J., Su, J., Cui, T., Li, X., Dong, X., Sun, F., Yang, Y., Tong, D., Zheng, Y., Li, Y., Li, J., Zhang, Q., and He, K.: Dominant role of emission reduction in $PM_{2.5}$ air quality improvement in Beijing during 2013–2017: a model-based decomposition analysis, Atmos. Chem. Phys., 19, 6125–6146, https://doi.org/10.5194/acp-19-6125-2019, 2019.

Cheng, Y., Zheng, G., Wei, C., Mu, Q., Zheng, B., Wang, Z., Gao, M., Zhang, Q., He, K., Carmichael, G., Pöschl, U., and Su, H.: Reactive nitrogen chemistry in aerosol water as a source of sulfate during haze events in China, Sci. Adv., 2, e1601530, https://doi.org/10.1126/sciadv.1601530, 2016.

Clegg, S. L., Brimblecombe, P., and Wexler, A. S.: Thermodynamic Model of the System $H^+-NH_4^+-Na^+-SO_4^{2-}-NO_3^--Cl^--H_2O$ at 298.15 K, J. Phys. Chem. A, 102, 2155–2171, https://doi.org/10.1021/jp973043j, 1998.

Clifton, C. L., Altstein, N., and Huie, R. E.: Rate constant for the reaction of nitrogen dioxide with sulfur(IV) over the pH range 5.3–13, Environ. Sci. Technol., 22, 586–589, https://doi.org/10.1021/es00170a018, 1988.

Cooney, D. O., Kim, S.-S., and Davis, E. J.: Analyses of mass transfer in hemodialyzers for laminar blood flow and homogeneous dialysate, Chem. Eng. Sci., 29, 1731–1738, https://doi.org/10.1016/0009-2509(74)87031-4, 1974.

Cui, R., Guo, X., Deng, F., and Liu, H.: Analysis of Water-soluble Ions and Elements in PM_{10} and $PM_{2.5}$, J. Environ. Health, 25, 291–294, https://doi.org/10.16241/j.cnki.1001-5914.2008.04.001, 2008 (in Chinese).

Davis, R. D., Lance, S., Gordon, J. A., Ushijima, S. B., and Tolbert, M. A.: Contact efflorescence as a pathway for crystallization of atmospherically relevant particles, P. Natl. Acad. Sci. USA, 112, 15815–15820, https://doi.org/10.1073/pnas.1522860113, 2015.

Ding, J., Zhao, P., Su, J., Dong, Q., Du, X., and Zhang, Y.: Aerosol pH and its driving factors in Beijing, Atmos. Chem. Phys., 19, 7939–7954, https://doi.org/10.5194/acp-19-7939-2019, 2019.

Duan, J., Huang, R.-J., Lin, C., Dai, W., Wang, M., Gu, Y., Wang, Y., Zhong, H., Zheng, Y., Ni, H., Dusek, U., Chen, Y., Li, Y., Chen, Q., Worsnop, D. R., O'Dowd, C. D., and Cao, J.: Distinctions in source regions and formation mechanisms of secondary aerosol in Beijing from summer to winter, Atmos. Chem. Phys., 19, 10319–10334, https://doi.org/10.5194/acp-19-10319-2019, 2019.

Ervens, B.: Modeling the Processing of Aerosol and Trace Gases in Clouds and Fogs, Chem. Rev., 115, 4157–4198, https://doi.org/10.1021/cr5005887, 2015.

Fang, Y., Ye, C., Wang, J., Wu, Y., Hu, M., Lin, W., Xu, F., and Zhu, T.: Relative humidity and O_3 concentration as two prerequisites for sulfate formation, Atmos. Chem. Phys., 19, 12295–12307, https://doi.org/10.5194/acp-19-12295-2019, 2019.

Fröhlich, R., Cubison, M. J., Slowik, J. G., Bukowiecki, N., Prévôt, A. S. H., Baltensperger, U., Schneider, J., Kimmel, J. R., Gonin, M., Rohner, U., Worsnop, D. R., and Jayne, J. T.: The ToF-ACSM: a portable aerosol chemical speciation monitor with TOFMS detection, Atmos. Meas. Tech., 6, 3225–3241, https://doi.org/10.5194/amt-6-3225-2013, 2013.

Guo, H., Sullivan, A. P., Campuzano-Jost, P., Schroder, J. C., Lopez-Hilfiker, F. D., Dibb, J. E., Jimenez, J. L., Thornton, J. A., Brown, S. S., Nenes, A., and Weber, R. J.: Fine particle pH and the partitioning of nitric acid during winter in the northeastern United States, J. Geophys. Res.-Atmos., 121, 10355–10376, https://doi.org/10.1002/2016JD025311, 2016.

Guo, S., Hu, M., Zamora, M. L., Peng, J., Shang, D., Zheng, J., Du, Z., Wu, Z., Shao, M., Zeng, L., Molina, M. J., and Zhang, R.: Elucidating severe urban haze formation in China, P. Natl. Acad. Sci. USA, 111, 17373–17378, https://doi.org/10.1073/pnas.1419604111, 2014.

Han, C., Liu, Y., and He, H.: Role of Organic Carbon in Heterogeneous Reaction of NO_2 with Soot, Environ. Sci. Technol., 47, 3174–3181, https://doi.org/10.1021/es304468n, 2013.

He, H., Wang, Y., Ma, Q., Ma, J., Chu, B., Ji, D., Tang, G., Liu, C., Zhang, H., and Hao, J.: Mineral dust and NO_x promote the conversion of SO_2 to sulfate in heavy pollution days, Sci. Rep., 4, 4172, https://doi.org/10.1038/srep04172, 2014.

He, P., Alexander, B., Geng, L., Chi, X., Fan, S., Zhan, H., Kang, H., Zheng, G., Cheng, Y., Su, H., Liu, C., and Xie, Z.: Isotopic constraints on heterogeneous sulfate production in Beijing haze, Atmos. Chem. Phys., 18, 5515–5528, https://doi.org/10.5194/acp-18-5515-2018, 2018.

Hollaway, M., Wild, O., Yang, T., Sun, Y., Xu, W., Xie, C., Whalley, L., Slater, E., Heard, D., and Liu, D.: Photochemical impacts of haze pollution in an urban environment, Atmos. Chem. Phys., 19, 9699–9714, https://doi.org/10.5194/acp-19-9699-2019, 2019.

Hu, D. W., Chen, J. M., Ye, X. N., Li, L., and Yang, X.: Hygroscopicity and evaporation of ammonium chloride and ammonium nitrate: Relative humidity and size effects on the growth factor, Atmos. Environ., 45, 2349–2355, https://doi.org/10.1016/j.atmosenv.2011.02.024, 2011.

Huang, L., Zhao, Y., Li, H., and Chen, Z.: Kinetics of Heterogeneous Reaction of Sulfur Dioxide on Authentic Mineral Dust: Effects of Relative Humidity and Hydrogen Peroxide, Environ. Sci. Technol., 49, 10797–10805, https://doi.org/10.1021/acs.est.5b03930, 2015.

Huang, L., An, J., Koo, B., Yarwood, G., Yan, R., Wang, Y., Huang, C., and Li, L.: Sulfate formation during heavy winter haze events and the potential contribution from heterogeneous $SO_2 + NO_2$ reactions in the Yangtze River Delta region, China, Atmos. Chem. Phys., 19, 14311–14328, https://doi.org/10.5194/acp-19-14311-2019, 2019.

Huang, R.-J., Zhang, Y., Bozzetti, C., Ho, K.-F., Cao, J.-J., Han, Y., Daellenbach, K. R., Slowik, J. G., Platt, S. M., Canonaco, F., Zotter, P., Wolf, R., Pieber, S. M., Bruns, E. A., Crippa, M., Ciarelli, G., Piazzalunga, A., Schwikowski, M., Abbaszade, G., Schnelle-Kreis, J., Zimmermann, R., An, Z., Szidat, S., Baltensperger, U., Haddad, I. E., and Prévôt, A. S. H.: High secondary aerosol contribution to particulate pollution during haze events in China, Nature, 514, 218–222, https://doi.org/10.1038/nature13774, 2014.

Hung, H.-M., Hsu, M.-N., and Hoffmann, M. R.: Quantification of SO_2 oxidation on interfacial surfaces of acidic micro-droplets: Implication for ambient sulfate formation, Environ. Sci. Technol., 52, 9079–9086, https://doi.org/10.1021/acs.est.8b01391, 2018.

Ji, D., Gao, W., Maenhaut, W., He, J., Wang, Z., Li, J., Du, W., Wang, L., Sun, Y., Xin, J., Hu, B., and Wang, Y.: Impact of air pollution control measures and regional transport on carbonaceous aerosols in fine particulate matter in urban Beijing, China: insights gained from long-term measurement, Atmos. Chem. Phys., 19, 8569–8590, https://doi.org/10.5194/acp-19-8569-2019, 2019.

Kong, L. D., Zhao, X., Sun, Z. Y., Yang, Y. W., Fu, H. B., Zhang, S. C., Cheng, T. T., Yang, X., Wang, L., and Chen, J. M.: The effects of nitrate on the heterogeneous uptake of sulfur dioxide on hematite, Atmos. Chem. Phys., 14, 9451–9467, https://doi.org/10.5194/acp-14-9451-2014, 2014.

Kortelainen, A., Hao, L., P. Tiitta, P., Jaatinen, A., Miettinen, P., Kulmala, M., Smith, J., Laaksonen, A., Worsnop, D., and Virtanen, A.: Sources of particulate organic nitrates in the boreal forest in Finland, Boreal Environ. Res., 22, 13–26, 2017.

Kulmala, M., and Wagner, P. E.: Mass accommodation and uptake coefficients – a quantitative comparison, J. Aerosol Sci., 32, 833–841, https://doi.org/10.1016/S0021-8502(00)00116-6, 2001.

Lang, J., Zhang, Y., Zhou, Y., Cheng, S., Chen, D., Guo, X., Chen, S., Li, X., Xing, X., and Wang, H.: Trends of PM2.5 and Chemical Composition in Beijing, 2000–2015, Aerosol Air Qual. Res., 17, 412–425, https://doi.org/10.4209/aaqr.2016.07.0307, 2017.

Lelieveld, J., Evans, J. S., Fnais, M., Giannadaki, D., and Pozzer, A.: The contribution of outdoor air pollution sources to premature mortality on a global scale, Nature, 525, 367–371, https://doi.org/10.1038/nature15371, 2015.

Li, C., Martin, R. V., van Donkelaar, A., Boys, B. L., Hammer, M. S., Xu, J.-W., Marais, E. A., Reff, A., Strum, M., Ridley, D. A., Crippa, M., Brauer, M., and Zhang, Q.: Trends in chemical composition of global and regional population-weighted fine particulate matter estimated for 25 Years, Environ. Sci. Technol., 51, 11185–11195, https://doi.org/10.1021/acs.est.7b02530, 2017.

Li, H., Zhang, Q., Zheng, B., Chen, C., Wu, N., Guo, H., Zhang, Y., Zheng, Y., Li, X., and He, K.: Nitrate-driven urban haze pollution during summertime over the North China Plain, Atmos. Chem. Phys., 18, 5293–5306, https://doi.org/10.5194/acp-18-5293-2018, 2018.

Li, Y. J., Liu, P. F., Bergoend, C., Bateman, A. P., and Martin, S. T.: Rebounding hygroscopic inorganic aerosol particles: Liquids, gels, and hydrates, Aerosol Sci. Technol., 51, 388–396, https://doi.org/10.1080/02786826.2016.1263384, 2017.

Lightstone, J. M., Onasch, T. B., Imre, D., and Oatis, S.: Deliquescence, Efflorescence, and Water Activity in ammonium nitrate and mixed ammonium nitrate/succinic acid microparticles, J. Phys. Chem. A, 104, 9337–9346, https://doi.org/10.1021/jp002137h, 2000.

Liu, C., Ma, Q., Liu, Y., Ma, J., and He, H.: Synergistic reaction between SO_2 and NO_2 on mineral oxides: a potential formation pathway of sulfate aerosol, Phys. Chem. Chem. Phys., 14, 1668–1676, https://doi.org/10.1039/C1CP22217A, 2012.

Liu, F., Beirle, S., Zhang, Q., van der A, R. J., Zheng, B., Tong, D., and He, K.: NO_x emission trends over Chinese cities estimated from OMI observations during 2005 to 2015, Atmos. Chem. Phys., 17, 9261–9275, https://doi.org/10.5194/acp-17-9261-2017, 2017.

Liu, H., He, K., Wang, Q., Huo, H., Lents, J., Davis, N., Nikkila, N., Chen, C., Osses, M., and He, C.: Comparison of vehicle activity and emission inventory between Beijing and Shanghai, J. Air Waste Manage. Assoc., 57, 1172–1177, https://doi.org/10.3155/1047-3289.57.10.1172, 2007.

Liu, L., Bei, N., Wu, J., Liu, S., Zhou, J., Li, X., Yang, Q., Feng, T., Cao, J., Tie, X., and Li, G.: Effects of stabilized Criegee intermediates (sCIs) on sulfate formation: a sensitivity analysis during summertime in Beijing–Tianjin–Hebei (BTH), China, Atmos. Chem. Phys., 19, 13341–13354, https://doi.org/10.5194/acp-19-13341-2019, 2019.

Liu, P., Ye, C., Xue, C., Zhang, C., Mu, Y., and Sun, X.: Formation mechanisms of atmospheric nitrate and sulfate during the winter haze pollution periods in Beijing: gas-phase, heterogeneous and aqueous-phase chemistry, Atmos. Chem. Phys., 20, 4153–4165, https://doi.org/10.5194/acp-20-4153-2020, 2020.

Liu, T., Clegg, S. L., and Abbatt, J. P. D.: Fast oxidation of sulfur dioxide by hydrogen peroxide in deliquesced aerosol particles, P. Natl. Acad. Sci. USA, 117, 1354–1359, https://doi.org/10.1073/pnas.1916401117, 2020.

Liu, T., Chan, A. W. H., and Abbatt, J. P. D.: Multiphase oxidation of sulfur dioxide in aerosol particles: implications for sulfate formation in polluted environments, Environ. Sci. Technol., 55, 4227–4242, https://doi.org/10.1021/acs.est.0c06496, 2021.

Liu, Y., Liggio, J., Harner, T., Jantunen, L., Shoeib, M., and Li, S.-M.: Heterogeneous OH initiated oxidation: A possible explanation for the persistence of organophosphate flame retardants in air, Environ. Sci. Technol., 48, 1041–1048, https://doi.org/10.1021/es404515k, 2014.

Liu, Y., Han, C., Ma, J., Bao, X., and He, H.: Influence of relative humidity on heterogeneous kinetics of NO_2 on kaolin and hematite, Phys. Chem. Chem. Phys., 17, 19424–19431, https://doi.org/https://doi.org/10.1039/C5CP02223A, 2015.

Liu, Y., Wu, Z., Wang, Y., Xiao, Y., Gu, F., Zheng, J., Tan, T., Shang, D., Wu, Y., Zeng, L., Hu, M., Bateman, A. P., and Martin, S. T.: Submicrometer particles are in the liquid state during heavy haze episodes in the urban atmosphere of Beijing, China, Environ. Sci. Technol. Lett., 4, 427–432, https://doi.org/10.1021/acs.estlett.7b00352, 2017.

Liu, Y., Wu, Z., Huang, X., Shen, H., Bai, Y., Qiao, K., Meng, X., Hu, W., Tang, M., and He, L.: Aerosol phase state and its link to chemical composition and liquid water content in a subtropical coastal megacity, Environ. Sci. Technol., 53, 5027–5033, https://doi.org/10.1021/acs.est.9b01196, 2019.

Liu, Y., Ni, S., Jiang, T., Xing, S., Zhang, Y., Bao, X., Feng, Z., Fan, X., Zhang, L., and Feng, H.: Influence of Chinese New Year overlapping COVID-19 lockdown on HONO sources in Shijiazhuang, Sci. Total Environ., 745, 141025, https://doi.org/10.1016/j.scitotenv.2020.141025, 2020a.

Liu, Y., Yan, C., Feng, Z., Zheng, F., Fan, X., Zhang, Y., Li, C., Zhou, Y., Lin, Z., Guo, Y., Zhang, Y., Ma, L., Zhou, W., Liu, Z., Wei, Z., Dada, L., Dallenbach, K. R., Kontkanen, J., Cai, R., Chan, T., Chu, B., Du, W., Yao, L., Wang, Y., Cai, J., Kangasluoma, J., Kokkonen, T., Kujansuu, J., Rusanen, A., Deng, C., Fu, Y., Yin, R., Li, X., Lu, Y., Liu, Y., Lian, C., Yang, D., Wang, W., Ge, M., Wang, Y., Worsnop, D., Junninen, H., He, H., Kerminen, V. M., Zheng, J., Wang, L., Jiang, J., Petäjä, T., Bianchi, F., and Kulmala, M.: Continuous and comprehensive atmospheric observations in Beijing: A station to understand the complex urban atmospheric environment, Big Earth Data, 4, 295–321, https://doi.org/10.1080/20964471.2020.1798707, 2020b.

Liu, Y., Zhang, Y., Lian, C., Yan, C., Feng, Z., Zheng, F., Fan, X., Chen, Y., Wang, W., Chu, B., Wang, Y., Cai, J., Du, W., Daellenbach, K. R., Kangasluoma, J., Bianchi, F., Kujansuu, J., Petäjä, T., Wang, X., Hu, B., Wang, Y., Ge, M., He, H., and Kulmala, M.: The promotion effect of nitrous acid on aerosol formation in wintertime in Beijing: the possible contribution of traffic-related emissions, Atmos. Chem. Phys., 20, 13023–13040, https://doi.org/10.5194/acp-20-13023-2020, 2020c.

Ma, Q., Liu, Y., and He, H.: Synergistic effect between NO_2 and SO_2 in their adsorption and reaction on γ-alumina, J. Phys. Chem. A, 112, 6630–6635, https://doi.org/10.1021/jp802025z, 2008.

Maaß, F., Elias, H., and Wannowius, K. J.: Kinetics of the oxidation of hydrogen sulfite by hydrogen peroxide in aqueous solution: ionic strength effects and temperature dependence, At-

mos. Environ., 33, 4413–4419, https://doi.org/10.1016/S1352-2310(99)00212-5, 1999.

Maahs, H. G.: Kinetics and mechanism of the oxidation of S(IV) by ozone in aqueous solution with particular reference to SO_2 conversion in nonurban tropospheric clouds, J. Geophys. Res.-Oceans, 88, 10721–10732, https://doi.org/10.1029/JC088iC15p10721, 1983.

Marshall, F. H., Berkemeier, T., Shiraiwa, M., Nandy, L., Ohm, P. B., Dutcher, C. S., and Reid, J. P.: Influence of particle viscosity on mass transfer and heterogeneous ozonolysis kinetics in aqueous–sucrose–maleic acid aerosol, Phys. Chem. Chem. Phys., 20, 15560–15573, https://doi.org/10.1039/C8CP01666F, 2018.

Martin, L. R. and Good, T. W.: Catalyzed oxidation of sulfur dioxide in solution: The iron-manganese synergism, Atmos. Environ. A-Gen., 25, 2395–2399, https://doi.org/10.1016/0960-1686(91)90113-L, 1991.

Murphy, D. M. and Fahey, D. W.: Mathematical treatment of the wall loss of a trace species in denuder and catalytic converter tubes, Anal. Chem., 59, 2753–2759, https://doi.org/10.1021/ac00150a006, 1987.

Onasch, T. B., Siefert, R. L., Brooks, S. D., Prenni, A. J., Murray, B., Wilson, M. A., and Tolbert, M. A.: Infrared spectroscopic study of the deliquescence and efflorescence of ammonium sulfate aerosol as a function of temperature, J. Geophys. Res.-Atmos., 104, 21317–21326, https://doi.org/10.1029/1999jd900384, 1999.

Pye, H. O. T., Nenes, A., Alexander, B., Ault, A. P., Barth, M. C., Clegg, S. L., Collett Jr., J. L., Fahey, K. M., Hennigan, C. J., Herrmann, H., Kanakidou, M., Kelly, J. T., Ku, I.-T., McNeill, V. F., Riemer, N., Schaefer, T., Shi, G., Tilgner, A., Walker, J. T., Wang, T., Weber, R., Xing, J., Zaveri, R. A., and Zuend, A.: The acidity of atmospheric particles and clouds, Atmos. Chem. Phys., 20, 4809–4888, https://doi.org/10.5194/acp-20-4809-2020, 2020.

Qi, J., Zheng, B., Li, M., Yu, F., Chen, C., Liu, F., Zhou, X., Yuan, J., Zhang, Q., and He, K.: A high-resolution air pollutants emission inventory in 2013 for the Beijing-Tianjin-Hebei region, China, Atmos. Environ., 170, 156–168, https://doi.org/10.1016/j.atmosenv.2017.09.039, 2017.

Ravishankara, A. R.: Heterogeneous and multiphase chemistry in the troposphere, Science, 276, 1058–1065, https://doi.org/10.1126/science.276.5315.1058, 1997.

Seinfeld, J. H. and Pandis, S. N.: Atmospheric chemistry and physics: From air pollution to climate change, 2nd Edn., John Wiley and Sons, New Jersey, USA, 429–44, 2006.

Shao, J., Chen, Q., Wang, Y., Lu, X., He, P., Sun, Y., Shah, V., Martin, R. V., Philip, S., Song, S., Zhao, Y., Xie, Z., Zhang, L., and Alexander, B.: Heterogeneous sulfate aerosol formation mechanisms during wintertime Chinese haze events: air quality model assessment using observations of sulfate oxygen isotopes in Beijing, Atmos. Chem. Phys., 19, 6107–6123, https://doi.org/10.5194/acp-19-6107-2019, 2019.

Shi, G., Xu, J., Shi, X., Liu, B., Bi, X., Xiao, Z., Chen, K., Wen, J., Dong, S., Tian, Y., Feng, Y., Yu, H., Song, S., Zhao, Q., Gao, J., and Russell, A. G.: Aerosol pH dynamics during haze periods in an urban environment in China: Use of detailed, hourly, speciated observations to study the role of ammonia availability and secondary aerosol formation and urban environment, J. Geophys. Res.-Atmos., 124, 9730–9742, https://doi.org/10.1029/2018JD029976, 2019.

Shiraiwa, M., Ammann, M., Koop, T., and Pöschl, U.: Gas uptake and chemical aging of semisolid organic aerosol particles, P. Natl. Acad. Sci. USA, 108, 11003–11008, https://doi.org/10.1073/pnas.1103045108, 2011.

Shiraiwa, M., Li, Y., Tsimpidi, A. P., Karydis, V. A., Berkemeier, T., Pandis, S. N., Lelieveld, J., Koop, T., and Pöschl, U.: Global distribution of particle phase state in atmospheric secondary organic aerosols, Nat. Commun., 8, 15002, https://doi.org/10.1038/ncomms15002, 2017.

Song, Q. and Osada, K.: Seasonal variation of aerosol acidity in Nagoya, Japan and factors affecting it, Atmos. Environ. X, 5, 100062, https://doi.org/10.1016/j.aeaoa.2020.100062, 2020.

Spindler, G., Hesper, J., Brüggemann, E., Dubois, R., Müller, T., and Herrmann, H.: Wet annular denuder measurements of nitrous acid: laboratory study of the artefact reaction of NO_2 with S(IV) in aqueous solution and comparison with field measurements, Atmos. Environ., 37, 2643–2662, https://doi.org/10.1016/S1352-2310(03)00209-7, 2003.

Sun, J., Liu, L., Xu, L., Wang, Y., Wu, Z., Hu, M., Shi, Z., Li, Y., Zhang, X., Chen, J., and Li, W.: Key Role of Nitrate in Phase Transitions of Urban Particles: Implications of Important Reactive Surfaces for Secondary Aerosol Formation, J. Geophys. Res.-Atmos., 123, 1234–1243, https://doi.org/10.1002/2017jd027264, 2018.

Sun, Y. L., Wang, Z. F., Du, W., Zhang, Q., Wang, Q. Q., Fu, P. Q., Pan, X. L., Li, J., Jayne, J., and Worsnop, D. R.: Long-term real-time measurements of aerosol particle composition in Beijing, China: seasonal variations, meteorological effects, and source analysis, Atmos. Chem. Phys., 15, 10149–10165, https://doi.org/10.5194/acp-15-10149-2015, 2015.

Tang, G., Zhang, J., Zhu, X., Song, T., Münkel, C., Hu, B., Schäfer, K., Liu, Z., Zhang, J., Wang, L., Xin, J., Suppan, P., and Wang, Y.: Mixing layer height and its implications for air pollution over Beijing, China, Atmos. Chem. Phys., 16, 2459–2475, https://doi.org/10.5194/acp-16-2459-2016, 2016.

Tian, M., Liu, Y., Yang, F. M., Zhang, L. M., Peng, C., Chen, Y., Shi, G. M., Wang, H. B., Luo, B., Jiang, C. T., Li, B., Takeda, N., and Koizumi, K.: Increasing importance of nitrate formation for heavy aerosol pollution in two megacities in Sichuan Basin, southwest China, Environ. Pollut., 250, 898–905, https://doi.org/10.1016/j.envpol.2019.04.098, 2019.

Tilgner, A., Schaefer, T., Alexander, B., Barth, M., Collett Jr., J. L., Fahey, K. M., Nenes, A., Pye, H. O. T., Herrmann, H., and McNeill, V. F.: Acidity and the multiphase chemistry of atmospheric aqueous particles and clouds, Atmos. Chem. Phys. Discuss. [preprint], https://doi.org/10.5194/acp-2021-58, in review, 2021.

Usher, C. R., Michel, A. E., and Grassian, V. H.: Reactions on mineral dust, Chem. Rev., 103, 4883–4939, https://doi.org/10.1021/cr020657y, 2003.

Wand, M. P. and Jones, M. C.: Comparison of smoothing parameterizations in bivariate kernel density estimation, J. Am. Stat. Assoc., 88, 520–528, https://doi.org/10.1080/01621459.1993.10476303, 1993.

Wang, G., Zhang, R., Gomez, M. E., Yang, L., Zamora, M. L., Hu, M., Lin, Y., Peng, J., Guoc, S., Meng, J., Li, J., Cheng, C., Hu, T., Ren, Y., Wang, Y., Gao, J., Cao, J., An, Z., Zhou, W., Li, G.,

Wang, J., Tian, P., Marrero-Ortiz, W., Secrest, J., Du, Z., Zheng, J., Shang, D., Zeng, L., Shao, M., Wang, W., Huang, Y., Wang, Y., Zhu, Y., Li, Y., Hu, J., Pan, B., Cai, L., Cheng, Y., Ji, Y., Zhang, F., Rosenfeld, D., Liss, P. S., Duce, R. A., Kolb, C. E., and Molina, M. J.: Persistent sulfate formation from London Fog to Chinese haze, P. Natl. Acad. Sci. USA, 113, 13630–13635, https://doi.org/10.1073/pnas.1616540113, 2016.

Wang, J. F., Li, J. Y., Ye, J. H., Zhao, J., Wu, Y. Z., Hu, J. L., Liu, D. T., Nie, D. Y., Shen, F. Z., Huang, X. P., Huang, D. D., Ji, D. S., Sun, X., Xu, W. Q., Guo, J. P., Song, S. J., Qin, Y. M., Liu, P. F., Turner, J. R., Lee, H. C., Hwang, S. W., Liao, H., Martin, S. T., Zhang, Q., Chen, M. D., Sun, Y. L., Ge, X. L., and Jacob, D. J.: Fast sulfate formation from oxidation of SO_2 by NO_2 and HONO observed in Beijing haze, Nat. Commun., 11, 2844, https://doi.org/10.1038/s41467-020-16683-x, 2020.

Wang, Q.-Q., Ma, Y.-L., Tan, J.-H., Yang, F.-M., Wei, L.-F., Duan, J.-C., and He, K.-B.: Characterization of water-soluble heavy metals of $PM_{2.5}$ during winter in Beijing, China Environ. Sci., 34, 2204–2210, 2014 (in Chinese).

Wang, W., Liu, M., Wang, T., Song, Y., Zhou, L., Cao, J., Hu, J., Tang, G., Chen, Z., Li, Z., Xu, Z., Peng, C., Lian, C., Chen, Y., Pan, Y., Zhang, Y., Sun, Y., Li, W., Zhu, T., Tian, H., and Ge, M.: Sulfate formation is dominated by manganese-catalyzed oxidation of SO_2 on aerosol surfaces during haze events, Nat. Commun., 12, 1993, https://doi.org/10.1038/s41467-021-22091-6, 2021.

Wang, Y., Zhuang, G., Tang, A., Yuan, H., Sun, Y., Chen, S., and Zheng, A.: The ion chemistry and the source of $PM_{2.5}$ aerosol in Beijing, Atmos. Environ., 39, 3771–3784, https://doi.org/10.1016/j.atmosenv.2005.03.013, 2005.

Wang, Y., Chen, Y., Wu, Z., Shang, D., Bian, Y., Du, Z., Schmitt, S. H., Su, R., Gkatzelis, G. I., Schlag, P., Hohaus, T., Voliotis, A., Lu, K., Zeng, L., Zhao, C., Alfarra, M. R., McFiggans, G., Wiedensohler, A., Kiendler-Scharr, A., Zhang, Y., and Hu, M.: Mutual promotion between aerosol particle liquid water and particulate nitrate enhancement leads to severe nitrate-dominated particulate matter pollution and low visibility, Atmos. Chem. Phys., 20, 2161–2175, https://doi.org/10.5194/acp-20-2161-2020, 2020.

Wang, Y. S., Teter, J., and Sperling, D.: China's soaring vehicle population: Even greater than forecasted?, Energ. Policy, 39, 3296–3306, https://doi.org/10.1016/j.enpol.2011.03.020, 2011.

Warneck, P.: The oxidation of sulfur(IV) by reaction with iron(III): A critical review and data analysis, Phys. Chem. Chem. Phys., 20, 4020–4037, https://doi.org/10.1039/C7CP07584G, 2018.

World Health Organization (WHO): Air quality guidelines – global update 2005, World Health Organization, Geneva, Switzerland, 11, available at: https://www.euro.who.int (last access: 27 August 2021), 2006.

World Health Organization (WHO): Health effects of particulate matter, World Health Organization, Geneva, Switzerland, 7, available at: https://www.euro.who.int (last access: 27 August 2021), 2013.

Wu, L., Sun, J., Zhang, X., Zhang, Y., Wang, Y., Zhong, J., and Yang, Y.: Aqueous-phase reactions occurred in the $PM_{2.5}$ cumulative explosive growth during the heavy pollution episode (HPE) in 2016 Beijing wintertime, Tellus B, 71, 1620079, https://doi.org/10.1080/16000889.2019.1620079, 2019.

Wu, Z., Wang, Y., Tan, T., Zhu, Y., Li, M., Shang, D., Wang, H., Lu, K., Guo, S., Zeng, L., and Zhang, Y.: Aerosol liquid water driven by anthropogenic inorganic salts: Implying its key role in haze formation over the North China Plain, Environ. Sci. Technol. Lett., 5, 160–166, https://doi.org/10.1021/acs.estlett.8b00021, 2018.

Xie, Y., Ding, A., Nie, W., Mao, H., Qi, X., Huang, X., Xu, Z., Kerminen, V.-M., Petäjä, T., Chi, X., Virkkula, A., Boy, M., Xue, L., Guo, J., Sun, J., Yang, X.-Q., Kulmala, M., and Fu, C.: Enhanced sulfate formation by nitrogen dioxide: Implications from in-situ observations at the SORPES Station, J. Geophys. Res.-Atmos., 120, 12679–12694, https://doi.org/10.1002/2015JD023607, 2015.

Xue, J., Yuan, Z., Griffith, S. M., Yu, X., Lau, A. K. H., and Yu, J. Z.: Sulfate formation enhanced by a cocktail of high NO_x, SO_2, particulate matter, and droplet pH during haze-fog events in megacities in China: An observation-based modeling investigation, Environ. Sci. Technol., 50, 7325–7334, https://doi.org/10.1021/acs.est.6b00768, 2016.

Yang, D., Zhang, S., Niu, T., Wang, Y., Xu, H., Zhang, K. M., and Wu, Y.: High-resolution mapping of vehicle emissions of atmospheric pollutants based on large-scale, real-world traffic datasets, Atmos. Chem. Phys., 19, 8831–8843, https://doi.org/10.5194/acp-19-8831-2019, 2019.

Yang, W., He, H., Ma, Q., Ma, J., Liu, Y., Liu, P., and Mu, Y.: Synergistic formation of sulfate and ammonium resulting from reaction between SO_2 and NH_3 on typical mineral dust, Phys. Chem. Chem. Phys., 18, 956–964, https://doi.org/10.1039/C5CP06144J, 2016.

Yao, L., Fan, X., Yan, C., Kurtén, T., Daellenbach, K., Li, C., Wang, Y., Guo, Y., Dada, L., Rissanen, M. P., Cai, J., Tham, Y. J., Zha, Q., Zhang, S., Du, W., Yu, M., Zheng, F., Zhou, Y., Kontkanen, J., Chan, T., Shen, J., Kujansuu, J. T., Kangasluoma, J., Jiang, J., Wang, L., Worsnop, D. R., Petäjä, T., Kerminen, V.-M., Liu, Y., Chu, B., He, H., Kulmala, M., and Bianchi, F.: Unprecedented ambient sulphur trioxide (SO_3) detection: Possible formation mechanism and atmospheric implications, Environ. Sci. Technol. Lett., 7, 809–818, https://doi.org/10.1021/acs.estlett.0c00615, 2020.

Ye, C., Liu, P., Ma, Z., Xue, C., Zhang, C., Zhang, Y., Liu, J., Liu, C., Sun, X., and Mu, Y.: High H_2O_2 concentrations observed during haze periods during the winter in Beijing: Importance of H_2O_2 oxidation in sulfate formation, Environ. Sci. Technol. Lett., 5, 757–763, https://doi.org/10.1021/acs.estlett.8b00579, 2018.

Ye, C., Chen, H., Hoffmann, E. H., Mettke, P., Tilgner, A., He, L., Mutzel, A., Brüggemann, M., Poulain, L., Schaefer, T., Heinold, B., Ma, Z., Liu, P., Xue, C., Zhao, X., Zhang, C., Zhang, F., Sun, H., Li, Q., Wang, L., Yang, X., Wang, J., Liu, C., Xing, C., Mu, Y., Chen, J., and Herrmann, H.: Particle-phase photoreactions of HULIS and TMIs establish a strong source of H_2O_2 and particulate sulfate in the winter North China Plain, Environ. Sci. Technol., 55, 7818–7830, https://doi.org/10.1021/acs.est.1c00561, 2021.

Yu, Z., Jang, M., and Park, J.: Modeling atmospheric mineral aerosol chemistry to predict heterogeneous photooxidation of SO_2, Atmos. Chem. Phys., 17, 10001–10017, https://doi.org/10.5194/acp-17-10001-2017, 2017.

Zhang, F., Wang, Y., Peng, J., Chen, L., Sun, Y., Duan, L., Ge, X., Li, Y., Zhao, J., Liu, C., Zhang, X., Zhang, G., Pan, Y., Wang, Y., Zhang, A. L., Ji, Y., Wang, G., Hu, M., Molina, M. J., and Zhang, R.: An unexpected catalyst dominates formation and radiative forcing of regional haze, P. Natl. Acad. Sci. USA, 117, 3960–3966, https://doi.org/10.1073/pnas.1919343117, 2020.

Zhang, X., Zhong, J., Wang, J., Wang, Y., and Liu, Y.: The interdecadal worsening of weather conditions affecting aerosol pollution in the Beijing area in relation to climate warming, Atmos. Chem. Phys., 18, 5991–5999, https://doi.org/10.5194/acp-18-5991-2018, 2018.

Zhang, Y., Sun, J., Zhang, X., Shen, X., Wang, T., and Qin, M.: Seasonal characterization of components and size distributions for submicron aerosols in Beijing, Sci. China Earth Sci., 56, 890–900, https://doi.org/10.1007/s11430-012-4515-z, 2013.

Zhang, Y., Bao, F., Li, M., Chen, C., and Zhao, J.: Nitrate enhanced oxidation of SO_2 on mineral dust: A vital role of proton, Environ. Sci. Technol., 53, 10139–10145, https://doi.org/10.1021/acs.est.9b01921, 2019.

Zhao, Y., Liu, Y., Ma, J., Ma, Q., and He, H.: Heterogeneous reaction of SO_2 with soot: The roles of relative humidity and surface composition of soot in surface sulfate formation, Atmos. Environ., 152, 465–476, https://doi.org/10.1016/j.atmosenv.2017.01.005, 2017.

Zheng, B., Zhang, Q., Zhang, Y., He, K. B., Wang, K., Zheng, G. J., Duan, F. K., Ma, Y. L., and Kimoto, T.: Heterogeneous chemistry: a mechanism missing in current models to explain secondary inorganic aerosol formation during the January 2013 haze episode in North China, Atmos. Chem. Phys., 15, 2031–2049, https://doi.org/10.5194/acp-15-2031-2015, 2015.

Zhong, J., Zhang, X., Dong, Y., Wang, Y., Liu, C., Wang, J., Zhang, Y., and Che, H.: Feedback effects of boundary-layer meteorological factors on cumulative explosive growth of $PM_{2.5}$ during winter heavy pollution episodes in Beijing from 2013 to 2016, Atmos. Chem. Phys., 18, 247–258, https://doi.org/10.5194/acp-18-247-2018, 2018.

Ziemke, J. R., Oman, L. D., Strode, S. A., Douglass, A. R., Olsen, M. A., McPeters, R. D., Bhartia, P. K., Froidevaux, L., Labow, G. J., Witte, J. C., Thompson, A. M., Haffner, D. P., Kramarova, N. A., Frith, S. M., Huang, L.-K., Jaross, G. R., Seftor, C. J., Deland, M. T., and Taylor, S. L.: Trends in global tropospheric ozone inferred from a composite record of TOMS/OMI/MLS/OMPS satellite measurements and the MERRA-2 GMI simulation , Atmos. Chem. Phys., 19, 3257–3269, https://doi.org/10.5194/acp-19-3257-2019, 2019.